

Flavor physics induced by light Z' from SO(10) GUT

Junji Hisano^{1,2,3}, Yu Muramatsu^{4,5}, Yuji Omura¹ and Yoshihiro Shigekami²

¹ *Kobayashi-Maskawa Institute for the Origin of Particles and the Universe,
Nagoya University, Nagoya 464-8602, Japan*

² *Department of Physics, Nagoya University, Nagoya 464-8602, Japan*

³ *Kavli IPMU (WPI), UTIAS, The University of Tokyo, Kashiwa,
Chiba 277-8583, Japan*

⁴ *School of Physics, KIAS, Seoul 130-722, Republic of Korea*

⁵ *Quantum Universe Center, KIAS, Seoul 130-722, Republic of Korea*

Abstract

In this paper, we investigate predictions of the SO(10) Grand Unified Theory (GUT), where an extra $U(1)'$ gauge symmetry remains up to the supersymmetry (SUSY) breaking scale. The minimal setup of SO(10) GUT unifies quarks and leptons into a **16**-representational field in each generations. The setup, however, suffers from the realization of the realistic Yukawa couplings at the electroweak scale. In order to solve this problem, we introduce **10**-representational matter fields, and then the two kinds of matter fields mix with each other at the SUSY breaking scale, where the extra $U(1)'$ gauge symmetry breaks down radiatively. One crucial prediction is that the Standard Model quarks and leptons are given by the linear combinations of the fields with two different $U(1)'$ charges. The mixing also depends on the flavor. Consequently, the $U(1)'$ interaction becomes flavor violating, and the flavor physics is the smoking-gun signal of our GUT model. The flavor violating Z' couplings are related to the fermion masses and the CKM matrix, so that we can derive some explicit predictions in flavor physics. We especially discuss $K-\bar{K}$ mixing, $B_{(s)}-\bar{B}_{(s)}$ mixing, and the (semi)leptonic decays of K and B in our model. We also study the flavor violating μ and τ decays and discuss the correlations among the physical observables in this SO(10) GUT framework.

1 Introduction

The supersymmetric SO(10) Grand Unified Theory (GUT) is one of the promising candidates for the underlying theory of the Standard Model (SM). The GUT elegantly explains the origin of the SM gauge groups and shows that the SM matter fields can be unified into three-family **16**-representational fields in the minimal SO(10) GUT [1]. In fact, several problems have been pointed out in the framework of the minimal setup, but the supersymmetric GUT deserves to be believed because of the beauty and the elegant explanations of the origins of not only the SM gauge groups but also the electroweak (EW) scale, so that a lot of solutions for the problems have been also proposed so far.

For instance, the unification of the SM matters, i.e. the unification of the Yukawa couplings, is a very attractive hypothesis, but unfortunately the precise experimental measurements of the masses and the CKM matrix require some deviation from the unified Yukawa couplings. One simple solution is to add higher-dimensional operators involving Higgs fields to break the SO(10) and SU(5) gauge symmetries [2].* In the minimal SO(10) GUT, there is only up-type Yukawa coupling, h_{ij} , at the renormalizable level, but realistic Yukawa couplings could be effectively obtained by including such a higher-dimensional operator contribution. However, we have to assume that the additional contributions and h_{ij} are compatible and cancel each other, in order to realize the large mass hierarchy between top and bottom quarks, if $\tan\beta$ is small. h_{tt} , which corresponds to the top quark mass is $\mathcal{O}(1)$, and then the effective term should be also $\mathcal{O}(1)$ for the bottom quark mass.

Another issue is how to achieve the Higgs mass observed around 125 GeV. In the supersymmetric GUT, the EW scale is naturally derived and the lightest Higgs mass is predicted. The lower bound on the predicted Higgs mass is roughly the Z boson mass and shifted by the supersymmetry (SUSY) breaking scale. In order to achieve the 125 GeV mass, it is known that the SUSY breaking scale should be $\mathcal{O}(100)$ TeV [5], unless the SUSY spectrum is unique (e.g. see Refs. [6–9]). In this high-scale SUSY scenario, however, the problem about the Yukawa couplings is revived because such $\mathcal{O}(100)$ TeV SUSY scale requires small $\tan\beta$ for the 125 GeV Higgs mass. Thus, we have to consider some mechanisms to realize the large mass hierarchy especially between top and bottom quarks, in order to avoid the remarkably large coefficients of higher-dimensional operators.

In Ref. [10], the authors propose an extension of the minimal SO(10) GUT to explain the hierarchy in the high-scale SUSY scenario. In addition to the **16** matter fields, three-family **10** fields are introduced and the realistic Yukawa couplings are achieved by the mixing between two kinds of SU(5) $\bar{\mathbf{5}}$ -representational fields originated from **16** and **10** fields respectively. An interesting point is that Z' interaction, predicted by SO(10) gauge symmetry, becomes flavor-dependent because the SU(5) $\bar{\mathbf{5}}$ -representational fields carry different U(1)' charges [10]. Once we assume that U(1)' is radiatively broken at the SUSY scale as the EW scale is, the flavor violating processes triggered by Z' are verifiable in the flavor experiments, such as the LHCb, the Belle II, the COMET and the Mu2e experiments.†

*Introducing additional Higgs fields [3] and additional matter fields [4] have been proposed so far.

†Introduction of additional matter multiplets at low energy enhances proton decay by X -boson ex-

In this paper, we investigate our predictions of the flavor violating couplings quantitatively and discuss the flavor violating processes relevant to our SO(10) GUT. Especially, all elements of our Flavor Changing Neutral Currents (FCNCs) involving Z' become large so that we should carefully check the consistencies with the observables related to the first and second generations: K - \bar{K} mixing and lepton flavor violating μ decays. Besides, we find that the (b, s) element of the Z' couplings tends to be larger than the others because of the fermion masses, as we will see in Sec. 2.2. Then, we study B physics as well: $B_{(s)}$ - $\bar{B}_{(s)}$ mixing, $B_{(s)} \rightarrow \mu^+\mu^-$ and so on. We also show our prediction on $K_L \rightarrow \pi\nu\bar{\nu}$ motivated by the KOTO experiment. Then, we discuss lepton flavor violations (LFV) in our model. Interestingly, we could find some correlations between the observables of mesons and leptons. Then, we show our predictions for $\mu \rightarrow 3e$ and the μ - e conversion in nuclei.

Our paper is organized as follows. In Sec. 2, we give a short review on our setup, based on Ref. [10]. Then, we show how well the realistic Yukawa couplings can be achieved and discuss our prediction of the Z' FCNCs in Sec. 2.1. In Sec. 3, we study flavor physics in our SO(10) GUT, concentrating on the relevant processes: K - \bar{K} mixing, $B_{(s)}$ - $\bar{B}_{(s)}$ mixing, $\mu \rightarrow 3e$, and so on. We give some analyses on $\Delta F = 1$ processes as well, but we will conclude that ϵ_K gives the strongest bound on our model. We also show the correlation between ϵ_K and LFV μ decays: $\mu \rightarrow 3e$ and μ - e conversion in nuclei in Sec. 3.3. Then, we see that our model could be tested at the COMET and the Mu2e experiments near future. Finally, we present some results for LFV τ decays in Sec. 3.4. Sec. 4 is devoted to summary.

2 Overview of the setup

In the minimal setup of the SO(10) GUT, the matter superfields belong to the $\mathbf{16}$ representation and the Yukawa couplings are described by one 3×3 matrix, h_{ij} :

$$W_{\min} = h_{ij} \mathbf{16}_i \mathbf{16}_j \mathbf{10}_H, \quad (1)$$

where $i, j = 1, 2, 3$ denote the generations and $\mathbf{10}_H$ is the chiral superfield for the Higgs. $\mathbf{16}_i$ includes all quarks and leptons in each generations, so that it is hard for this minimal setup to describe the mass hierarchies in the each sectors and the CKM matrix.

In Ref. [10], the authors propose a simple setup of the SO(10) GUT to realize the realistic Yukawa couplings at the EW scale. We introduce three $\mathbf{10}$ -representational chiral superfields ($\mathbf{10}_i$) in addition to $\mathbf{16}_i$. Then we write down the additional Yukawa couplings and mass terms for $\mathbf{10}_i$:

$$W_{\text{ex}} = g_{ij} \mathbf{16}_i \mathbf{10}_j \mathbf{16}_H + \mu_{10ij} \mathbf{10}_i \mathbf{10}_j. \quad (2)$$

$\mathbf{16}_H$ is an extra Higgs field to break the remaining $U(1)'$ symmetry. In order to sketch our idea, let us focus on the down-type quark sector, assuming that SO(10)-adjoint chiral

change, since the gauge coupling constants at the GUT scale become larger [11]. If proton decay is discovered, embedding quarks and leptons to GUT multiplets may be resolved.

superfields, $\mathbf{45}_H$ and $\mathbf{45}'_H$, break $\text{SO}(10)$ to $\text{G}_{\text{SM}} \times \text{U}(1)'$ at the GUT scale. There are two kinds of right-handed down-type quarks which carry different $\text{U}(1)'$ charges, after the symmetry breaking: $d_{L,Ri}^{(16)}$, and $d_{L,Ri}^{(10)}$, which are originated from the $\mathbf{16}_i$ and $\mathbf{10}_i$. Involving the scalar component (Φ) of the SM singlet in $\mathbf{16}_H$, we find the 6×6 mass matrixes for the down-type quarks induced by $W_{\text{min}} + W_{\text{ex}}$:

$$\mathcal{L}_d = -\overline{\begin{pmatrix} d_{Ri}^{(16)} & d_{Ri}^{(10)} \end{pmatrix}} \begin{pmatrix} h_{ij}v_d & g_{ij}\langle\Phi\rangle \\ 0 & \mu_{10ij} \end{pmatrix} \begin{pmatrix} d_{Lj}^{(16)} \\ d_{Lj}^{(10)} \end{pmatrix}, \quad (3)$$

where v_d denotes the nonzero VEV of the down-type Higgs doublet belonging to $\mathbf{10}_H$. As we see in Eq. (3), if Φ develops nonzero VEV, $d_i^{(16)}$ and $d_i^{(10)}$ mix with each other and the lightest three down-type quarks can be interpreted as the SM down-type quarks. Note that Φ is charged under $\text{U}(1)'$, so that non-vanishing VEV of Φ spontaneously breaks $\text{U}(1)'$.

Let us define the mixing as follows:

$$\begin{pmatrix} d_R \\ d_R^h \end{pmatrix} = U_d \begin{pmatrix} d_R^{(16)} \\ d_R^{(10)} \end{pmatrix} = \begin{pmatrix} \hat{U}_{16}^d & \Delta U_d \\ \Delta U_d' & \hat{U}_{10}^d \end{pmatrix} \begin{pmatrix} d_R^{(16)} \\ d_R^{(10)} \end{pmatrix}, \quad (4)$$

where d_R is the right-handed SM quark and d_R^h is the extra heavy quark. In Eq. (4), the flavor index, i , is omitted. U_d is a 6×6 unitary matrix, and $\hat{U}_{16,10}^d$ and $\Delta U_d^{(\prime)}$ are 3×3 matrices that satisfy, for instance,

$$(\hat{U}_{16}^d)_{ik}(\hat{U}_{16}^{d*})_{jk} + (\Delta U_d)_{ik}(\Delta U_d^*)_{jk} = \delta_{ij}. \quad (5)$$

The mixing unitary matrix, U_d , is fixed by the parameters in the W_{ex} , following Eqs. (3) and (4). Now, let us simply consider the mixing in the limit that $h_{ij}v_d$ are much smaller than $g_{ij}\langle\Phi\rangle$ and μ_{10ij} . Then, the left-handed SM quarks are given by $d_{Li}^{(16)}$ ($\equiv d_{Li}$). The mixing for the right-handed quarks is given by the equation,

$$(\hat{U}_{16}^d)_{ik}g_{kj}\langle\Phi\rangle + (\Delta U_d)_{ik}\mu_{10kj} = 0. \quad (6)$$

Using the \hat{U}_{16}^d parameters, the Yukawa couplings (h_{ij}^d) to generate the SM down-type quark mass matrix is given by

$$h_{ij}^d = (\hat{U}_{16}^d)_{ik}h_{kj}. \quad (7)$$

h_{ij} is expected to explain the up-type SM quark mass matrix, so that \hat{U}_{16}^d matrix should be fitted to realized the mass hierarchy between the up-type and down-type quarks. However, it is difficult for h_{ij}^d to be realistic because of the relation in Eq. (5). The elements of \hat{U}_{16}^d could be $\mathcal{O}(1)$, but cannot be too large because of the unitary condition. As discussed in Ref. [10], the mass hierarchy between top and bottom quarks can be achieved, but the other mass relations and the CKM matrix especially involving the first and second generations require too large $(\hat{U}_{16}^d)_{ij}$, because of the very light up quark mass. In order

to complement the suppression factors, one can introduce higher-dimension operators involving $\mathbf{45}_H$ and $\mathbf{45}'_H$ fields and modify the relation in Eq. (7) as

$$h_{ij}^d = (\hat{U}_{16}^d)_{ik}(h_{kj}^u + \epsilon c_{kj}^d). \quad (8)$$

ϵ denotes the suppression factor from the ratio between the VEVs of $\mathbf{45}_H$ and $\mathbf{45}'_H$ and the unknown cut-off scale where the higher-dimensional operators are induced. h_{ij}^u are the Yukawa couplings for the up-type SM quarks and slightly deviated from h_{ij} , because of the higher-dimensional operators. c_{ij}^d are the free parameters in our model, and assumed to be $\mathcal{O}(1)$.

In the same manner, we can discuss the lepton sector. If the SU(5) relation is respected approximately, the Yukawa couplings (h_{ij}^l) for the charged lepton masses are given by h_{ij}^d . The experimental results, however, require slight SU(5) symmetry breaking effects. Then we introduce

$$h_{ij}^l = (\hat{U}_{16}^l)_{ik}(h_{kj}^u + \epsilon c_{kj}^l), \quad (9)$$

where \hat{U}_{16}^l is the 3×3 matrix which satisfies the relation in Eq. (5), replacing d with l . In principle, \hat{U}_{16}^d and \hat{U}_{16}^l (c_{ij}^d and c_{ij}^l) are different from each other, because the effective couplings generated by the VEVs of $\mathbf{45}_H$ and $\mathbf{45}'_H$ are different. We could expect that the corrections of the higher-dimensional operators are sufficiently small in the effective g_{ij} and μ_{10ij} couplings, and then it would be reasonable to assume

$$(\hat{U}_{16}^l)_{ij} \simeq (\hat{U}_{16}^d)_{ij}. \quad (10)$$

In this case, the realistic Yukawa couplings are achieved by $\epsilon c_{ij}^{d,l}$.

2.1 Requirements for the realistic Yukawa couplings

The up-type quark Yukawa couplings h_{ij}^u are defined as follows, without loss of generality:

$$h_{ij}^u = \frac{m_i^u}{v^u} \delta_{ij}, \quad (11)$$

where v^u is the VEV of the up-type Higgs doublet and m_i^u are the up-type quark masses, respectively. According to Eqs. (8) and (9), we find the equations which should be satisfied by the mixing parameters and coefficients of higher-dimensional operators:

$$h_{ij}^d = \frac{m_i^d}{v^d} (V_{CKM}^*)_{ji} = (\hat{U}_{16}^d)_{ik} \left(\frac{m_k^u}{v^u} \delta_{kj} + \epsilon c_{kj}^d \right), \quad (12)$$

$$h_{ij}^l = \frac{m_i^l}{v^d} (V_R^*)_{ji} = (\hat{U}_{16}^l)_{ik} \left(\frac{m_k^u}{v^u} \delta_{kj} + \epsilon c_{kj}^l \right), \quad (13)$$

where v^d is the VEV of the down-type Higgs doublet and m_i^d (m_i^l) are the down-type quark (lepton) masses, respectively. V_R is the unitary matrix and identical to the CKM matrix (V_{CKM}) in the SU(5) limit. The other constraints on the matrices, $\hat{U}_{16}^{d,l}$ and $c^{d,l}$, are from Eq. (5) and the perturbativity.

Note that heavy modes are integrated out around the $U(1)'$ breaking scale, and then $h_{ij}^{d,l}$ in Eqs. (8) and (9) are generated. In order to compare our predictions with the observed values of quark and lepton masses and CKM matrix, we need include the RG corrections from the $U(1)'$ breaking scale ($\mathcal{O}(100)$ TeV) to the low scale, e.g. the EW scale (M_Z).

We evaluate the realistic Yukawa couplings at the $U(1)'$ breaking scale ($M_{Z'}$) from the central values of the experimental measurements summarized in Table 1. There are three scales relevant to our scenario: M_Z , gluino mass (around 1 TeV), and $M_{Z'}$. First, we evolve the input parameters in Table 1 into the ones at the M_Z scale. We use Mathematica package RunDec [12] to evaluate the running quark masses. We translate lepton pole masses to $\overline{\text{MS}}$ running masses at the M_Z scale, following Ref. [13]. In our analysis, the up-type Yukawa coupling is defined as the diagonal form at M_Z , using the up-type quark masses. The down-type Yukawa coupling is given by the CKM matrix and the down-type quark.[‡] Next, we drive the Yukawa matrices from the M_Z scale to 1 TeV, using the SM RG running at the two-loop level [13]. We assume that all gaugino mass reside around 1 TeV, so that we convert the $\overline{\text{MS}}$ scheme into the $\overline{\text{DR}}$ scheme at 1 TeV according to Ref. [14] and drive the Yukawa matrices from 1 TeV scale to 100 TeV scale, including the gaugino contributions. In our scenario, the other SUSY particles reside around 100 TeV. As a result, we obtain the following values at 100 TeV:

$$\begin{aligned} (m_i^u) &= (8.4 \times 10^{-4} \text{ GeV}, 0.43 \text{ GeV}, 1.2 \times 10^2 \text{ GeV}), \\ (m_i^d) &= (1.9 \times 10^{-3} \text{ GeV}, 3.8 \times 10^{-2} \text{ GeV}, 1.9 \text{ GeV}), \\ (m_i^l) &= (5.0 \times 10^{-4} \text{ GeV}, 0.11 \text{ GeV}, 1.8 \text{ GeV}), \end{aligned} \quad (14)$$

and

$$V_{CKM} = \begin{pmatrix} 9.7 \times 10^{-1} & 2.3 \times 10^{-1} & 1.5 \times 10^{-3} - 3.6 \times 10^{-3}i \\ -2.3 \times 10^{-1} - 1.6 \times 10^{-4}i & 9.7 \times 10^{-1} & 4.4 \times 10^{-2} \\ 8.5 \times 10^{-3} - 3.5 \times 10^{-3}i & -4.3 \times 10^{-2} - 8.2 \times 10^{-4}i & 1.0 \end{pmatrix}. \quad (15)$$

Note that the quark and lepton masses, m_i^f ($f = u, d, l$), at 100 TeV are obtained, multiplying the running Yukawa couplings by $v = 174$ GeV. h_{ij}^f at 100 TeV are given by Eqs. (11), (12), and (13), taking $\tan \beta$ into account. In the next subsection, $(\hat{U}_{16}^d)_{ij}$ and $(\hat{U}_{16}^l)_{ij}$ are calculated, using the obtained h_{ij}^f and the relations in Eqs. (12) and (13).

2.2 Flavor violating Z' couplings

As we see in Eq. (4), the SM right-handed down-type quarks and left-handed leptons are given by the linear combinations of the parts of $\mathbf{16}_i$ and $\mathbf{10}_i$ in the $SO(10)$ GUT. We consider the scenario that an extra $U(1)'$ symmetry remains up to the SUSY breaking

[‡]In fact, we can multiply arbitral unitary matrices to define the Yukawa couplings. When we match our predictions with the realistic Yukawa couplings, we do not take such degrees of freedom into account.

m_e	0.5110 MeV [15]	λ	$0.22543_{-0.00031}^{+0.00042}$ [16]
m_μ	105.7 MeV [15]	A	$0.8227_{-0.0136}^{+0.0066}$ [16]
m_τ	1.777 GeV [15]	$\bar{\rho}$	$0.1504_{-0.0062}^{+0.0121}$ [16]
$m_d(2 \text{ GeV})$	$4.8_{-0.3}^{+0.5}$ MeV [15]	$\bar{\eta}$	$0.3540_{-0.0076}^{+0.0069}$ [16]
$m_s(2 \text{ GeV})$	95 ± 5 MeV [15]	M_Z	91.1876(21) GeV [15]
$m_b(m_b)$	4.18 ± 0.03 GeV [15]	M_W	80.385(15) GeV [15]
$\frac{2m_s}{(m_u+m_d)}(2 \text{ GeV})$	27.5 ± 1.0 [15]	$\sin^2 \theta_W$	0.23126(5) [15]
$m_c(m_c)$	1.275 ± 0.025 GeV [15]	G_F	$1.1663787(6) \times 10^{-5} \text{ GeV}^{-2}$ [15]
m_t	$173.21 \pm 0.51 \pm 0.71$ GeV [15]	α	1/137.036 [15]
		$\alpha_s(M_Z)$	0.1193(16) [15]

Table 1: The input parameters in our analysis. The CKM matrix, V_{CKM} , is written in terms of λ , A , $\bar{\rho}$ and $\bar{\eta}$ [15].

scale. Then, we find that the particles from $\mathbf{16}_i$ and $\mathbf{10}_i$ carry different $U(1)'$ charges corresponding to the representations of $SO(10)$. In fact, the $U(1)'$ charges of $d_{Ri}^{(16)}$ and $d_{Ri}^{(10)}$ are -3 and 2 , respectively, and the ones of $l_{Li}^{(16)}$ and $l_{Li}^{(10)}$ are 3 and -2 [10]. The $U(1)'$ symmetry breaking is triggered by the nonzero VEV of Φ , and causes the mixing between the different- $U(1)'$ -charged fields. Consequently, the Z' interaction becomes flavor violating as follows:

$$\mathcal{L}_g = g' \hat{Z}'_\mu \left(A_{ij}^l \bar{l}_L^i \gamma^\mu l_L^j - A_{ij}^d \bar{d}_R^i \gamma^\mu d_R^j - \bar{q}_L^i \gamma^\mu q_L^i + \bar{u}_R^i \gamma^\mu u_R^i + \bar{e}_R^i \gamma^\mu e_R^i \right), \quad (16)$$

where q_L^i , u_R^i and e_R^i are the mass eigenstates of the left-handed quarks, right-handed up-type quarks and right-handed charged leptons. Note that \hat{Z}'_μ is not the mass eigenstate. This mixes with the Z boson, as mentioned below. $A_{ij}^{l,d}$ are given by

$$A_{ij}^d = 5(\hat{U}_{16}^d)_{ik}(\hat{U}_{16}^d)_{jk}^* - 2\delta_{ij}, \quad A_{ij}^l = 5(\hat{U}_{16}^l)_{ik}^*(\hat{U}_{16}^l)_{jk} - 2\delta_{ij}. \quad (17)$$

Assuming the $SU(5)$ relation in Eq. (10), A_{ij}^d and A_{ij}^l satisfy

$$A_{ij}^d \simeq (A_{ij}^l)^*. \quad (18)$$

Figs. 1, 2 and 3 show our predictions. In the all figures of this paper, $\tan \beta$ is fixed at $\tan \beta = 3$ and the results in Eqs. (14) and (15) are used. In this calculation we assume that V_R is the CKM matrix. The red (blue) points correspond to arbitral complex $\epsilon c_{ij}^{d,l}$ satisfying $|\epsilon c_{ij}^{d,l}| < 10^{-2}$ ($|\epsilon c_{ij}^{d,l}| < 10^{-3}$).

Fig. 1 shows our prediction for A_{sd}^d and A_{dd}^d , which face the stringent bounds from $K-\bar{K}$ mixing. If we assume the GUT relation in Eq. (18), those elements are constrained

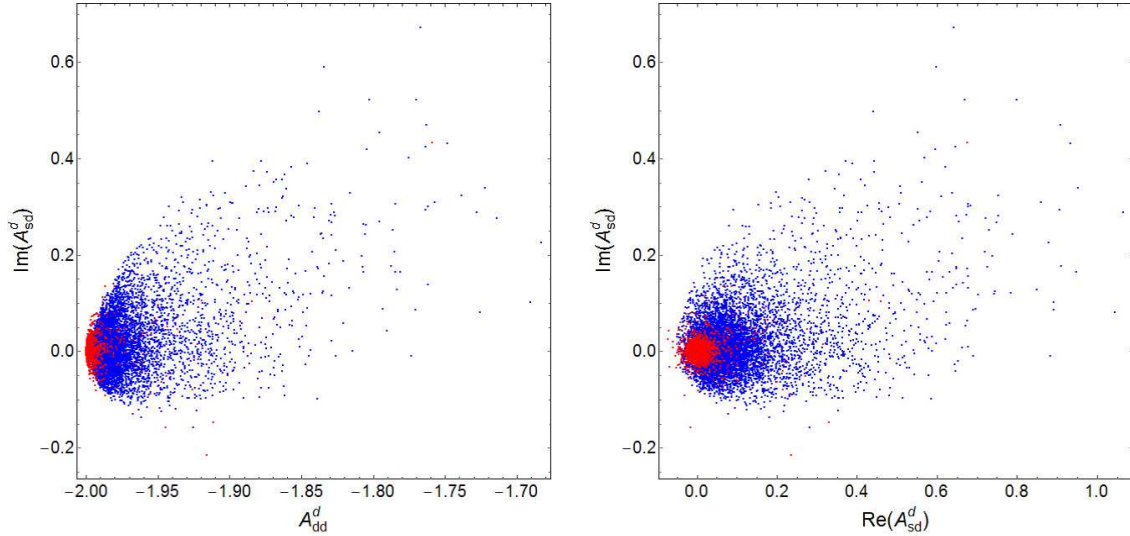


Figure 1: Our predictions for A_{dd}^d (left) and A_{sd}^d (right). The coefficients of higher-dimensional operators satisfy $|\epsilon c_{ij}^d| < 10^{-2}$ (red) and $|\epsilon c_{ij}^d| < 10^{-3}$ (blue).

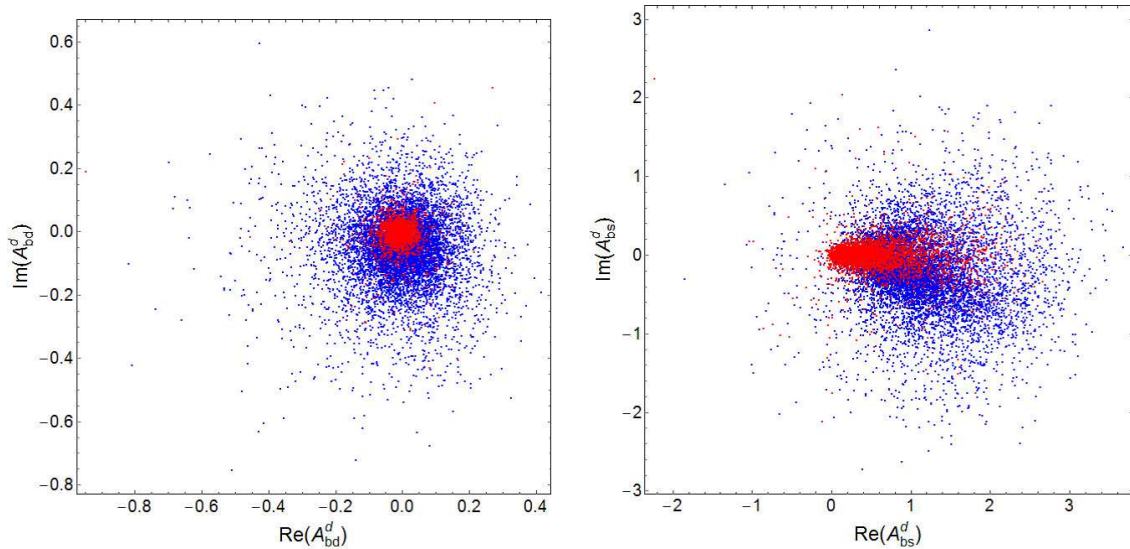


Figure 2: Our predictions for A_{bd}^d (left) and A_{bs}^d (right). The coefficients of higher-dimensional operators satisfy $|\epsilon c_{ij}^d| < 10^{-2}$ (red) and $|\epsilon c_{ij}^d| < 10^{-3}$ (blue).

by $\mu \rightarrow 3e$ and μ - e conversion in nuclei as well. As we see in Fig. 1, large A_{sd}^d is predicted, so we carefully study the K physics and μ physics in Sec. 3.

Let us comment on the mixing to realize the realistic Yukawa coupling. In the left panel of Fig. 1, A_{dd}^d is approximately estimated as $A_{dd}^d \simeq -2$, i.e. $(\hat{U}_{16}^d)_{1k}(\hat{U}_{16}^d)^*_{1k} \ll 1$. This means that the SM down quark mainly comes from the **10**-representational fields of

SO(10). The reason is as follows. We have introduced the higher dimensional operators, suppressed by ϵ , in order to compensate the small up quark mass. In fact, the contribution to the (1, 1) element of the up-type quark mass matrix, denoted by $v_u \epsilon c_{11}^d$, is larger than the up quark mass. Then, the down quark mass is roughly given by the suppressed $(\hat{U}_{16}^d)_{11}$ according to Eq. (12).

On the other hand, it seems that **10**- and **16**-representational fields mix with each other in the second and third generations, as in Figs. 1 and 2. A_{sd}^d is relatively smaller than the other off-diagonal elements, but could be $\mathcal{O}(0.1)$ according to the sizable $(\hat{U}_{16}^d)_{ij}$. We find that A_{bs}^d tend to be larger than the other FCNC couplings, in Figs. 1 and 2. This is because A_{ij}^d is proportional to the down-type quark masses, m_i^d and m_j^d ($i, j = d, s, b$), so roughly speaking, the ratios of $|A_{bs}^d/A_{sd}^d|$ and $|A_{bs}^d/A_{bd}^d|$ are $\mathcal{O}(m_b^d/m_d^d)$ and $\mathcal{O}(m_s^d/m_d^d)$, respectively, although the dependences of the quark masses and the CKM elements on $|A_{ij}^d|$ are not so simple. When ϵ is small, the approximate expressions for the flavor violating couplings are

$$\begin{aligned} \text{Re}(A_{sd}^d) &\sim 5 \tan^2 \beta \frac{m_d^d m_s^d}{|v_u \epsilon c_{11}^d|^2} \lambda, \quad \text{Im}(A_{sd}^d) \sim 5 \tan^2 \beta \frac{m_d^d m_s^d}{|v_u \epsilon c_{11}^d|^2} \text{Im} \left(\frac{v_u \epsilon c_{12}^{d*}}{m_c^u} \right), \\ A_{bd}^d &\sim 5 \tan^2 \beta \frac{m_d^d m_b^d}{|v_u \epsilon c_{11}^d|^2} \left(\frac{v_u \epsilon c_{12}^{d*}}{m_c^u} \right) A \lambda^2, \\ \text{Re}(A_{bs}^d) &\sim 5 \tan^2 \beta \frac{m_s^d m_b^d}{(m_c^u)^2} \lambda^2, \quad \text{Im}(A_{bs}^d) \sim 5 \tan^2 \beta \frac{m_s^d m_b^d}{|v_u \epsilon c_{11}^d|^2} \text{Im} \left(\frac{v_u \epsilon c_{12}^{d*}}{m_c^u} \right) A \lambda^3. \end{aligned} \quad (19)$$

These properties are the same for A_{ij}^l and then we expect that the ratio between $|A_{ij}^l|$ and $|A_{ij}^d|$ is predictive even if Eq. (10) is failed. When ϵ is small, the ratio is expected to be $\mathcal{O}(m_i^l m_j^l / (m_i^d m_j^d))$. Our prediction of the ratio is shown in Fig. 3. These figures show that these ratios tend to be close to the green diamond, which satisfies $|A_{ij}^l/A_{ij}^d| = m_i^l m_j^l / (m_i^d m_j^d)$, in the case with small ϵ . Especially, the convergence is remarkable in the (2, 1) elements, $|A_{\mu e}^l/A_{sd}^d|$.

In addition, \hat{Z}'_μ is the U(1)' gauge boson, but not the mass eigenstate because of mass mixing between \hat{Z}'_μ and Z boson denoted by \hat{Z}_μ . The mass mixing is generated by the U(1)'-charged Higgs doublets [10]:

$$\begin{pmatrix} \hat{Z}_\mu \\ \hat{Z}'_\mu \end{pmatrix} = \begin{pmatrix} \cos \theta & -\sin \theta \\ \sin \theta & \cos \theta \end{pmatrix} \begin{pmatrix} Z_\mu \\ Z'_\mu \end{pmatrix}, \quad (20)$$

where $\sin \theta$ is approximately estimated as

$$\tan 2\theta \simeq 4 \frac{g'}{g_Z} \frac{M_Z^2}{M_{Z'}^2}. \quad (21)$$

We have to include this effect, when we discuss the phenomenology in our model.

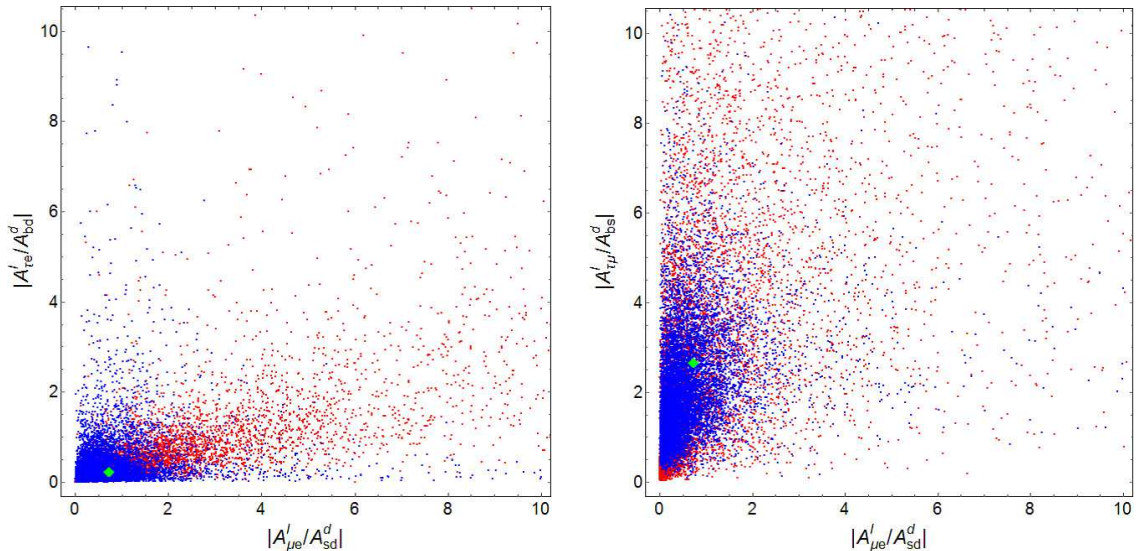


Figure 3: Our predictions for SU(5) relation. The coefficients of higher-dimensional operators satisfy $|\epsilon c_{ij}^{d,l}| < 10^{-2}$ (red) and $|\epsilon c_{ij}^{d,l}| < 10^{-3}$ (blue). Green diamond shows the value of each mass ratio of $m_i^l m_j^l / (m_i^d m_j^d)$.

Note that a scalar from Φ also has flavor changing Yukawa couplings with the SM fermions and the heavy extra fermions, but the left-handed down-type quarks (right-handed lepton) can be identified as the heavy fermions, because of the EW symmetry. Then, the flavor violating processes involving the scalar are loop-suppressed and negligibly small in our scenario.

3 Flavor Physics

In this section, we investigate the flavor violating signals predicted by our SO(10) GUT, based on the setup discussed above. One of the important predictions is that there are tree-level FCNCs involving Z'_μ and Z_μ . Moreover, all elements of the FCNCs could be $\mathcal{O}(1)$, corresponding to the higher-dimensional operators. This means that we have to seriously check the consistency with the flavor violating processes concerned with the first and second generations, such as $K-\bar{K}$ mixing and $\mu \rightarrow 3e$, because the processes are the most sensitive to the new physics contributions. Besides, we find that (b, s) element of the Z' coupling becomes larger than the other, so that we investigate the impact of our model on B physics, as well.

The SUSY particle contributions to FCNCs are suppressed by loop factors due to the R parity. However, when the flavor violation in squark mass terms is maximal, the SUSY contributions to the K system may not be negligible even if squark masses are $O(100)$ TeV. Then, we ignore them for simplicity.

First, we study the constraints from the $\Delta F = 2$ processes in K and $B_{(s)}$ systems

m_K	497.611(13) MeV [15]	m_{B_s}	5.3663(6) GeV [15]
F_K	156.1(11) MeV [18]	m_B	5.2795(3) GeV [15]
\hat{B}_K	0.764(10) [18]	F_{B_s}	227.7 ± 6.2 MeV [18]
$(\Delta M_K)_{\text{exp}}$	$3.484(6) \times 10^{-12}$ MeV [15]	F_B	190.6 ± 4.6 MeV [18]
$ \epsilon_K $	$(2.228(11)) \times 10^{-3}$ [15]	\hat{B}_{B_s}	1.33(6) [18]
$\text{BR}(K^+ \rightarrow \pi^0 e^+ \nu)$	5.07(4) % [15]	\hat{B}_B	1.26(11) [18]
$\tau(K^+)$	$(1.238(2)) \times 10^{-8}$ s [15]	η_B	0.55 [20]
$\tau(K_L)$	$(5.116(21)) \times 10^{-8}$ s [15]	η_Y	1.012 [39]
η_1	1.87(76) [19]	Γ_μ^{-1}	$2.1969811(22) \times 10^{-6}$ s
η_2	0.5765(65) [20]		
η_3	0.496(47) [21]		

Table 2: The input parameters relevant to our analyses in flavor physics.

in the next subsection, and then let us discuss the consistency of our model with the observations of the LFV μ decays in Sec. 3.3. We also study the $\Delta F = 1$ processes, although the constraints are mild.

3.1 $\Delta F = 2$ processes

In the SM, CP violation is caused by the CP phase in the CKM matrix. CP violating processes as well as flavor violating processes are strongly suppressed by the GIM mechanism, and the SM predictions are usually very tiny. The flavor processes of K meson are no exception. In fact, the SM prediction of K - \bar{K} mixing is quite small, but it is consistent with the experimental observations, although there are still sizable theoretical uncertainties in the SM predictions. In other words, large new physics contributions to the K physics conflict with the experimental results, and then the strong constraints should be taken into account. Similarly, we can derive the new physics constraints from B - \bar{B} and B_s - \bar{B}_s mixing.

In addition to the SM corrections, the $\Delta F = 2$ processes are caused by the tree-level FCNCs of Z' and Z in our model. The induced operators are

$$\mathcal{H}^{\Delta F=2} = \frac{1}{2} \sum_{q=K,B,B_s} \tilde{C}_1^q \tilde{Q}_1^q \quad (22)$$

where the each operator is given by

$$\tilde{Q}_1^K = (\bar{s}_R \gamma_\mu d_R)(\bar{s}_R \gamma^\mu d_R), \quad \tilde{Q}_1^B = (\bar{b}_R \gamma_\mu d_R)(\bar{b}_R \gamma^\mu d_R), \quad \tilde{Q}_1^{B_s} = (\bar{b}_R \gamma_\mu s_R)(\bar{b}_R \gamma^\mu s_R), \quad (23)$$

and the Wilson coefficient is estimated as

$$\tilde{C}_1^K = (A_{sd}^d)^2 \left(\frac{g'^2 \cos^2 \theta}{M_{Z'}^2} + \frac{g'^2 \sin^2 \theta}{M_Z^2} \right) \equiv \frac{(A_{sd}^d)^2}{\Lambda_{Z'}^2}. \quad (24)$$

\tilde{C}_1^B and $\tilde{C}_1^{B_s}$ can be derived by exchanging (A_{sd}^d) in \tilde{C}_1^K with (A_{bd}^d) and (A_{bs}^d) respectively. Note that the SM correction appears in the C_1^q ($q = K, B, B_s$), which are the coefficients of the operators that consist of only left-handed quarks, instead of the right-handed in \tilde{Q}_1^q : for example, $(\overline{s_L} \gamma_\mu d_L)(\overline{s_L} \gamma^\mu d_L)$. The CP-phase appears in the (t, d) -element of the CKM matrix in the SM. In our model, the FCNCs, A_{ij}^d , are generally complex, so that the CP-violating processes strongly constrain our Z' interaction.

In our analyses on flavor physics, we set $\Lambda_{Z'} = 1.4 \times 10^3$ TeV (500 TeV), which corresponds to $M_{Z'} = 100$ TeV (36 TeV) and $g' \simeq 0.073$ [10]. $\tan \beta$ is fixed at $\tan \beta = 3$ to achieve the 125 GeV Higgs mass [5].

3.1.1 $\Delta S = 2$ process

Based on Ref. [17], we investigate the upper bound on the Z' interaction from the K - \overline{K} mixing. The physical observables on the mixing are denoted by ϵ_K and ΔM_K , which are evaluated as

$$\epsilon_K = \frac{\kappa_\epsilon e^{i\varphi_\epsilon}}{\sqrt{2}(\Delta M_K)_{\text{exp}}} \text{Im}(M_{12}^K), \quad \Delta M_K = 2\text{Re}(M_{12}^K). \quad (25)$$

κ_ϵ and φ_ϵ are given by the observations: $\kappa_\epsilon = 0.94 \pm 0.02$ and $\varphi_\epsilon = 0.2417 \times \pi$. M_{12}^K is generated by the K - \overline{K} mixing and decomposed as follows in our model:

$$M_{12}^K = (M_{12}^K)_{\text{SM}} + \Delta M_{12}^K. \quad (26)$$

ΔM_{12}^K is the Z' contribution, and then it is given by

$$\Delta M_{12}^K = \frac{1}{2} \tilde{C}_1^K(\mu) \langle \tilde{Q}_1^K \rangle. \quad (27)$$

The matrix element, $\langle \tilde{Q}_1^K \rangle$, can be extracted from the SM prediction, because the only difference is the chirality. $\tilde{C}_1^K(\mu)$ is the Wilson coefficient derived from Eq. (24) and the RG correction. The running correction is studied in Appendix A.

The SM prediction is described as

$$(M_{12}^K)_{\text{SM}} = \frac{G_F^2}{12\pi^2} F_K^2 \hat{B}_K m_K M_W^2 \{ \lambda_c^2 \eta_1 S_0(x_c) + \lambda_t^2 \eta_2 S_0(x_t) + 2\lambda_c \lambda_t \eta_3 S(x_c, x_t) \}. \quad (28)$$

x_i and λ_i denote m_i^2/M_W^2 and $(V_{CKM})_{is}^*(V_{CKM})_{id}$, respectively. $\eta_{1,2,3}$ correspond to the NLO and NNLO QCD corrections [19–21]. The values we adopt are summarized in Table 2. The functions, $S_0(x_t)$ and $S(x_c, x_t)$, are shown in Appendix B.

The physical observables in K - \overline{K} mixing are experimentally measured well. On the other hand, the SM predictions still suffer from the large uncertainty from the matrix

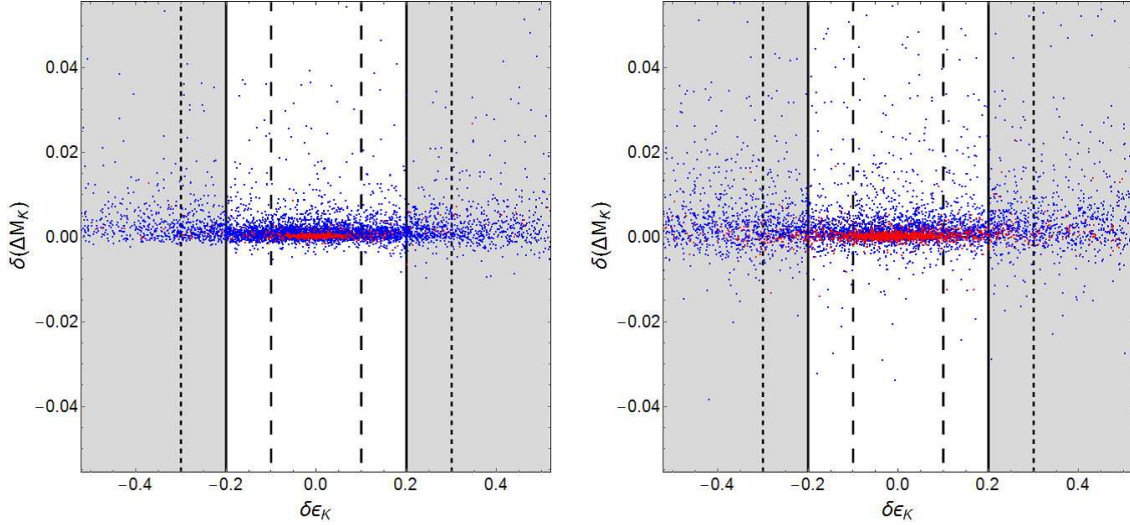


Figure 4: Our predictions for $\delta\epsilon_K$ and $\delta(\Delta M_K)$ with $\Lambda_{Z'} = 1400$ TeV (left) and $\Lambda_{Z'} = 500$ TeV (right). The coefficients of higher-dimensional operators satisfy $|\epsilon c_{ij}^d| < 10^{-2}$ (red) and $|\epsilon c_{ij}^d| < 10^{-3}$ (blue). Black dashed, solid and dotted line show the deviation from SM by 10%, 20% and 30%, respectively.

element and the CKM matrix. Using the central values in Table 1 and Table 2, we draw our predictions for the deviations of ϵ_K and ΔM_K from the SM predictions. Compared to the SM predictions, $(\epsilon_K)_{\text{SM}}$ and $(\Delta M_K)_{\text{SM}}$, the deviations are defined as

$$\delta\epsilon_K \equiv \epsilon_K/(\epsilon_K)_{\text{SM}} - 1 \quad \text{and} \quad \delta(\Delta M_K) \equiv \Delta M_K/(\Delta M_K)_{\text{SM}} - 1. \quad (29)$$

It is difficult to draw the exclusion limits in terms of $|\delta\epsilon_K|$ and $|\delta(\Delta M_K)|$, because of the large uncertainties of the SM predictions. In Ref. [22], the CKM fitter group shows that the experimental upper bounds on $|\delta\epsilon_K|$ and $|\delta(\Delta M_K)|$ are at most O(30) %. It will be developed up to O(20) % at the Belle II experiment [22].

In Fig. 4, our predictions for the deviations of ϵ_K and ΔM_K are shown in the cases with $\Lambda_{Z'} = 1400$ TeV (left) and $\Lambda_{Z'} = 500$ TeV (right). The black dashed, solid and dotted line show the deviation from SM by 10%, 20% and 30%, respectively. In our model, ϵ_K largely departs from the SM prediction, even if $\Lambda_{Z'}$ is $\mathcal{O}(10^3)$ TeV. Then, we have to consider the consistency with ϵ_K , whenever we discuss the other observables.

3.1.2 $\Delta B = 2$ process

We now derive our predictions of B - \bar{B} and B_s - \bar{B}_s mixing, as well as K - \bar{K} mixing. The observables relevant to the mixing are mass differences denoted by ΔM_B and ΔM_{B_s} . They are influenced by \tilde{C}_1^B and $\tilde{C}_1^{B_s}$ as follows:

$$\Delta M_{B_q} = 2 \left| (M_{12}^{B_q})_{\text{SM}} + \frac{1}{6} \tilde{C}_1^{B_q} m_{B_q} F_{B_q} \hat{B}_{B_q} \right| \quad (q = d, s), \quad (30)$$

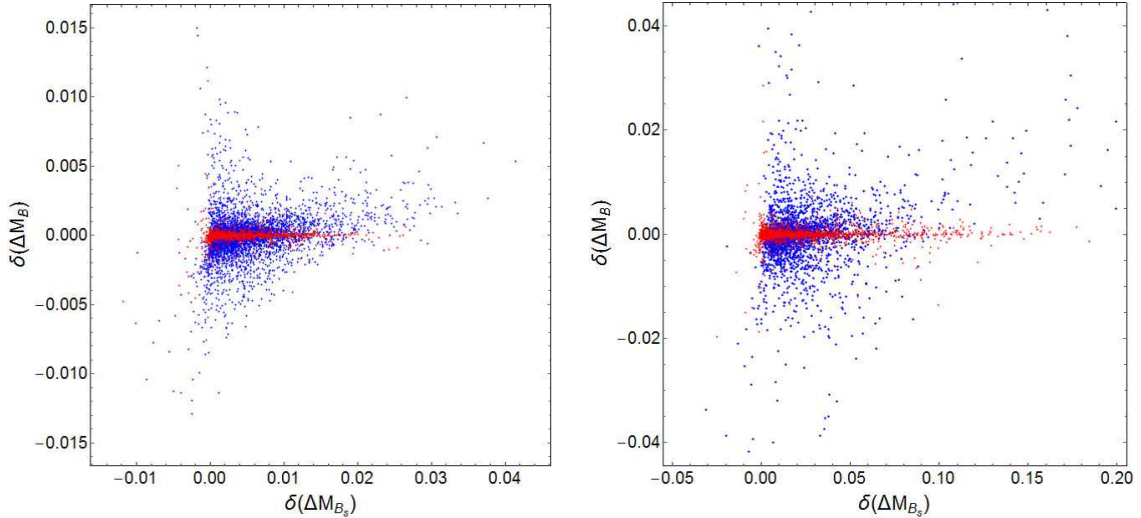


Figure 5: Our predictions for $\delta(\Delta M_{B_s})$ and $\delta(\Delta M_B)$ with $\Lambda_{Z'} = 1400$ TeV (left) and $\Lambda_{Z'} = 500$ TeV (right). The coefficients of higher-dimensional operators satisfy $|\epsilon c_{ij}^d| < 10^{-2}$ (red) and $|\epsilon c_{ij}^d| < 10^{-3}$ (blue). In these figures, we only show the points that $|\delta\epsilon_K| \leq 0.3$ is satisfied.

where $(M_{12}^{B_q})_{\text{SM}}$ is given by the top-loop contribution:

$$(M_{12}^{B_q})_{\text{SM}} = \frac{G_F^2}{12\pi^2} F_{B_q}^2 \hat{B}_{B_q} m_{B_q} M_W^2 \lambda_{B_q}^2 \eta_B S_0(x_t). \quad (31)$$

The input parameters used in our analyses are shown in Table 2. λ_{B_q} depicts $\lambda_{B_q} = (V_{CKM})_{tb}^* (V_{CKM})_{tq}$. The SM predictions still have large uncertainties dominated by the errors of hadronic mixing matrix elements and the CKM matrix elements, so that it would be difficult to draw the new physics constraints as well. Recently, the Fermilab and MILC Collaborations have shown their results on the SM predictions of ΔM_B and ΔM_{B_s} [23] and about 10 % errors are still inevitable. The LHCb and Belle II experiments will improve the measurement, as discussed in Ref. [22].

In our model, A_{bs}^d is large compared to the other elements, so that our model may be tested by ΔM_{B_s} , although the deviation is relatively smaller than the $K-\bar{K}$ mixing because of the size of the SM prediction. Fig. 5 shows our predictions for the deviations of ΔM_{B_s} and ΔM_B in the cases with $\Lambda_{Z'} = 1400$ TeV (left) and $\Lambda_{Z'} = 500$ TeV (right). These deviation are defined as the same manner in Eq. (29). If Z' is around $\mathcal{O}(10)$ TeV, $\delta(\Delta M_B)$ could reach 10 %, which maybe cause the tension with the current measurement [22]. In these figures, all points satisfy $|\delta\epsilon_K| \leq 0.3$.

3.2 $\Delta F = 1$ processes

The Z' interaction deviates the SM predictions in the rare decays of B and K mesons. The KOTO, Belle II and LHCb experiments will develop the measurements of the rare

decays and give some hints to new physics. In this section, we study the (semi) leptonic decays of K meson and the leptonic decays of B and B_s . The processes we especially study here are $K_L \rightarrow \pi^0 \nu \bar{\nu}$, measured by the KOTO experiment, $K_L \rightarrow \mu^+ \mu^-$, $\mu^\pm e^\mp$ and $B_s(B) \rightarrow \mu^+ \mu^-$.

3.2.1 $\Delta S = 1$ processes

The $\Delta S = 1$ processes, such as the rare K meson decays, play a crucial role in testing our model. The effective Hamiltonian which causes the tree-level flavor changing is given by the Z' exchanging and Z boson exchanging through the Z - Z' mixing:

$$\mathcal{H}^{\Delta S=1} = (C_I^f)_{ij} (\bar{s}_R \gamma_\mu d_R) (\bar{f}_I^i \gamma^\mu f_I^j), \quad (32)$$

where f denotes $f = \nu, l, u, d$ and I is the chirality of the fermions (f) ($I = L, R$). $(C_I^f)^{ij}$ at $\mu = M_{Z'}$ is described as

$$(C_I^f)_{ij} = -A_{sd}^d \left\{ \frac{(Q_I^f)_{ij}}{\Lambda_{Z'}^2} + \frac{\delta_{ij}}{\Lambda_Z^2} (\tau_I^f - Q_e^f \sin^2 \theta_W) \right\}, \quad (33)$$

where Λ_Z^2 is defined as

$$\frac{1}{\Lambda_Z^2} = g' g_Z \sin \theta \cos \theta \left(\frac{1}{M_Z^2} - \frac{1}{M_{Z'}^2} \right). \quad (34)$$

Note that the second term Λ_Z^2 is approximately evaluated as $\Lambda_Z^2 \simeq \Lambda_{Z'}^2/2$ according to Eq.(21), in the limit $M_{Z'} \gg M_Z$. $(Q_I^f)_{ij}$ are given by Eq. (16) as

$$((Q_L^{\nu,l})_{ij}, (Q_R^l)_{ij}) = (A_{ij}^l, +\delta_{ij}), \quad (35)$$

$$((Q_L^{u,d})_{ij}, (Q_R^u)_{ij}, (Q_R^d)_{ij}) = (-\delta_{ij}, +\delta_{ij}, -A_{ij}^d). \quad (36)$$

τ_I^f and Q_e^f are the isospin and the EW charge of f . In this subsection, we study the impacts of these new physics corrections on the K meson decays.

$K_L \rightarrow \pi^0 \nu \bar{\nu}$ and $K^+ \rightarrow \pi^+ \nu \bar{\nu}$

Another important measurement of the CP-violating processes is the rare decay of neutral K meson: $K_L \rightarrow \pi^0 \nu \bar{\nu}$. The SM prediction is quite tiny, and it is not still reached by the past and current experiments: $\text{BR}(K_L \rightarrow \pi^0 \nu \bar{\nu}) < 2.6 \times 10^{-8}$ [24]. The KOTO experiment at the J-PARC will cover the region near future. On the other hand, the decay of the charged K meson, $K^+ \rightarrow \pi^+ \nu \bar{\nu}$, has been already measured as $\text{BR}(K^+ \rightarrow \pi^+ \nu \bar{\nu}) = 1.73_{-1.05}^{+1.15} \times 10^{-10}$ [25] and will be updated by the NA62 experiment at the CERN.

In the SM, the both branching ratios are given by the following operators,

$$\mathcal{H}_{\text{SM}}^{\Delta S=1} = C_{\text{SM}} (\bar{s}_L \gamma_\mu d_L) (\bar{\nu}_L^i \gamma^\mu \nu_L^i). \quad (37)$$

C_{SM} is given by the Z penguin diagram and the box diagram involving W boson. Then, the SM prediction, C_{SM} , is described in the following form, [§]

$$C_{\text{SM}} = \frac{G_F}{\sqrt{2}} \frac{2\alpha}{\pi \sin^2 \theta_W} (\lambda_c X_c + \lambda_t X(x_t)). \quad (38)$$

$X_c/\lambda^4 = (0.42 \pm 0.03)$ is proposed in Ref. [17]. $X(x_t)$ is the short-distance contribution given by the Z -penguin diagrams and box diagrams involving top quark respectively. We can see the LO description in Appendix B. In addition, we have the Z' contribution to this process, as we see in Eqs. (32) and (33). Using the isospin symmetry and taking the ratio to $K^+ \rightarrow \pi^0 e^+ \nu$, the branching ratio of $K_L \rightarrow \pi^0 \nu \bar{\nu}$ is estimated as

$$\text{BR}(K_L \rightarrow \pi^0 \nu \bar{\nu}) = \frac{\mathcal{A}_{ij} \mathcal{A}_{ij}^*}{8|(V_{CKM})_{us}|^2 G_F^2} \times \frac{\tau(K_L)}{\tau(K^+)} \times r_{K_L} \times \text{BR}(K^+ \rightarrow \pi^0 e^+ \nu), \quad (39)$$

where \mathcal{A}_{ij} is defined as

$$\mathcal{A}_{ij} = \frac{1}{\sqrt{2}} \{ \delta_{ij} (C_{\text{SM}} - C_{\text{SM}}^*) + (C_L^\nu)_{ij} - (C_L^\nu)_{ji}^* \}. \quad (40)$$

r_{K_L} is the isospin breaking effect. Based on Ref. [27], we estimate it as $r_{K_L} \simeq 0.955$. Note that the SM prediction is $\text{BR}(K_L \rightarrow \pi^0 \nu \bar{\nu}) = 2.43(39)(6) \times 10^{-11}$ [28].

$K_L \rightarrow \pi^0 \nu \bar{\nu}$ is the CP-violating process, so that the decay depends on the imaginary part of the tree-level FCNCs. $\text{BR}(K^+ \rightarrow \pi^0 e^+ \nu)$ is well measured at the experiments, and we can expect that the Z' contribution to $K^+ \rightarrow \pi^0 e^+ \nu$ is rather small in this process. Then we use the experimental result as the input parameter. Note that the penguin diagram contribution to C_{SM} is also modified by $\cos^2 \theta$, but here we ignore such a new physics contribution at the one loop level.

Similarly, we can estimate the branching ratio of $K^+ \rightarrow \pi^+ \nu \bar{\nu}$,

$$\text{BR}(K^+ \rightarrow \pi^+ \nu \bar{\nu}) = \frac{\mathcal{A}_{ij}^+ \mathcal{A}_{ij}^{+*}}{8|(V_{CKM})_{us}|^2 G_F^2} \times r_{K^+} \times \text{BR}(K^+ \rightarrow \pi^0 e^+ \nu), \quad (41)$$

where \mathcal{A}_{ij}^+ is given by

$$\mathcal{A}_{ij}^+ = \sqrt{2} \{ \delta_{ij} C_{\text{SM}} + (C_L^\nu)_{ij} \}. \quad (42)$$

We estimate the isospin breaking effect, r_{K^+} , as $r_{K^+} \simeq 0.978$ [27]. Note that the SM prediction is $\text{BR}(K^+ \rightarrow \pi^+ \nu \bar{\nu}) = 7.81(75)(29) \times 10^{-11}$ [28].

Fig. 6 shows our predictions of $\text{BR}(K_L \rightarrow \pi^0 \nu \bar{\nu})$ and $\text{BR}(K^+ \rightarrow \pi^+ \nu \bar{\nu})$, satisfying $|\delta\epsilon_K| \leq 0.3$. Black solid lines show the SM predictions, using the center values in Table 2. $\text{BR}(K^+ \rightarrow \pi^+ \nu \bar{\nu})$ tends to be slightly larger than SM prediction. This is because this deviation is proportional to $\text{Re}(C_{\text{SM}} A_{sd}^d) \sim \text{Re}(C_{\text{SM}}) \text{Re}(A_{sd}^d)$, where $\text{Re}(A_{sd}^d)$ tends to be positive, as shown in Fig. 1 and Eq. (19). On the other hand, the dominant deviation of $\text{BR}(K_L \rightarrow \pi^0 \nu \bar{\nu})$ is proportional to $\text{Im}(C_{\text{SM}}) \text{Im}(A_{sd}^d)$. Therefore, such a specific trend can not be seen in $\text{BR}(K_L \rightarrow \pi^0 \nu \bar{\nu})$. In any case, our predictions do not largely depart from the SM prediction, as far as $\Lambda_{Z'} = 1.4 \times 10^3$ TeV. Even if $\Lambda_{Z'}$ is around 500 TeV, the deviation is at most 10 %, compared to the SM prediction.

[§]See Ref. [26] for the current status of the calculations.

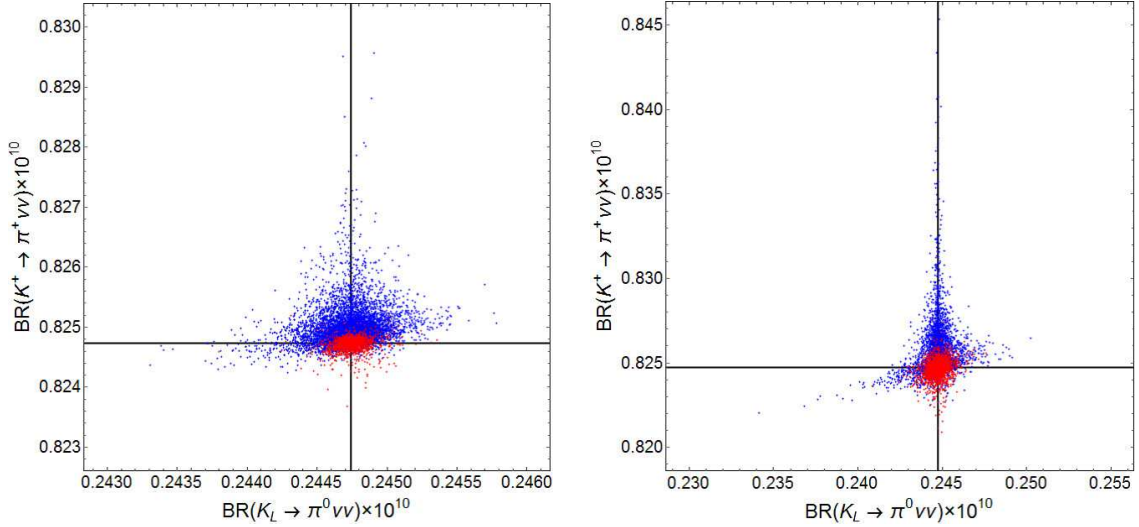


Figure 6: Our predictions for $\text{BR}(K_L \rightarrow \pi^0 \nu \bar{\nu})$ and $\text{BR}(K^+ \rightarrow \pi^+ \nu \bar{\nu})$ with $\Lambda_{Z'} = 1400$ TeV (left) and $\Lambda_{Z'} = 500$ TeV (right). The coefficients of higher-dimensional operators satisfy $|\epsilon c_{ij}^d| < 10^{-2}$ (red) and $|\epsilon c_{ij}^d| < 10^{-3}$ (blue). Black solid lines show each SM prediction. The all points satisfy $|\delta\epsilon_K| \leq 0.3$.

$K_L \rightarrow l_i l_j$ and $K_L \rightarrow \pi^0 l_i l_j$

The leptonic decays of K_L may be also important in our model. $K_L \rightarrow \mu^+ \mu^-$ has a large long-distance contribution in the decay width. In Ref. [29], the new physics constraint from $K_L \rightarrow \mu^+ \mu^-$ is proposed, extracting the the short-distance part: $\text{BR}(K_L \rightarrow \mu^+ \mu^-) < 2.5 \times 10^{-9}$. In our model, the branching ratio of $K_L \rightarrow \mu^+ \mu^-$ departs from the SM prediction because of the flavor changing Z' couplings. The extra contribution is depicted by $(C_{L,R}^l)_{\mu\mu}$ defined in Eq. (32). Following Refs. [17, 30, 31], we estimate the deviation of this leptonic decay. As we have already seen above, our prediction cannot be far from the SM one, as far as $\Lambda_{Z'} = \mathcal{O}(10^3)$ TeV. Then, the short-distance part of $\text{BR}(K_L \rightarrow \mu^+ \mu^-)$ is dominated by SM contribution, so that the ratio between our prediction and the SM one of $\text{BR}(K_L \rightarrow \mu^+ \mu^-)$ is estimated as

$$\left| \frac{\text{BR}(K_L \rightarrow \mu^+ \mu^-)}{\text{BR}(K_L \rightarrow \mu^+ \mu^-)_{\text{SM}}} - 1 \right| \leq 0.019, \quad (43)$$

when $\Lambda_{Z'} = 1.4 \times 10^3$ TeV. We conclude that the bound from this process does not threaten our model in the high-scale SUSY scenario.

The flavor violating decay of K_L has been experimentally investigated as well: $K_L \rightarrow \mu^+ e^- < 4.7 \times 10^{-12}$ [32]. Similarly, $\text{BR}(K_L \rightarrow \mu^+ e^-)$ also cannot be large in our model. Using $\Lambda_{Z'} = 1.4 \times 10^3$ TeV and typical values of A_{sd}^d and $A_{\mu e}^l$, this branching ratio is

$$\text{BR}(K_L \rightarrow \mu^+ e^-) \simeq 4.0 \times 10^{-19} \left(\frac{1400 \text{ TeV}}{\Lambda_{Z'}} \right)^4 \left(\frac{\text{Re}(A_{sd}^d)}{0.1} \right)^2 \left(\frac{|A_{\mu e}^l|}{0.04} \right)^2. \quad (44)$$

This is much below the experimental bound.

The semileptonic decay of K such as $K_L \rightarrow \pi^0 \bar{l}_i l_j$ may be relevant to our model. The current experimental upper bounds are [33, 34]

$$\text{BR}(K_L \rightarrow \pi^0 e^+ e^-) < 2.8 \times 10^{-10}, \quad (45)$$

$$\text{BR}(K_L \rightarrow \pi^0 \mu^+ \mu^-) < 3.8 \times 10^{-10}, \quad (46)$$

which are about 10 times bigger than the SM predictions [35], so that large new physics effects are still allowed in these decay modes. Similar to $K_L \rightarrow \mu^+ \mu^-$, $\text{BR}(K_L \rightarrow \pi^0 \bar{l} l)$ is dominated by SM contribution when $\Lambda_{Z'} = \mathcal{O}(10^3)$ TeV. Then, our predictions are below the experimental bounds.

The LFV decay of K_L , $K_L \rightarrow \pi^0 e^\mp \mu^\pm$, is also experimentally constrained as [36]

$$\text{BR}(K_L \rightarrow \pi^0 e^\mp \mu^\pm) < 7.6 \times 10^{-11}. \quad (47)$$

Using $\Lambda_{Z'} = 1.4 \times 10^3$ TeV and typical values of A_{sd}^d and $A_{\mu e}^l$, $\text{BR}(K_L \rightarrow \pi^0 e^- \mu^+)$ is

$$\text{BR}(K_L \rightarrow \pi^0 e^- \mu^+) \simeq 2.0 \times 10^{-20} \left(\frac{1400 \text{ TeV}}{\Lambda_{Z'}} \right)^4 \left(\frac{\text{Im}(A_{sd}^d)}{0.1} \right)^2 \left(\frac{|A_{\mu e}^l|}{0.04} \right)^2. \quad (48)$$

Thus, we conclude that our model is not threaten by this process, as far as $\Lambda_{Z'}$ is much bigger than $\mathcal{O}(10)$ TeV.

3.2.2 $B_s \rightarrow \mu^+ \mu^-$ and $B \rightarrow \mu^+ \mu^-$

In our model, there are large flavor violating Z' couplings in the (b, s) and (b, d) elements. Especially, A_{bs}^d tends to be large, as shown in Fig. 2. Then, the rare B_s decay would constrain our model strongly.

$B_s \rightarrow \mu^+ \mu^-$ and $B \rightarrow \mu^+ \mu^-$ have been measured at the LHC: $\text{BR}(B_s \rightarrow \mu^+ \mu^-) = 2.8_{-0.6}^{+0.7} \times 10^{-9}$ and $\text{BR}(B \rightarrow \mu^+ \mu^-) = 3.9_{-1.4}^{+1.5} \times 10^{-10}$ [37]. The SM predictions are $\text{BR}(B_s \rightarrow \mu^+ \mu^-) = (3.66 \pm 0.23) \times 10^{-9}$ and $\text{BR}(B \rightarrow \mu^+ \mu^-) = (1.06 \pm 0.09) \times 10^{-10}$ [38], which are almost consistent with the experimental results, although the errors are large. In our model, the both leptonic decays are deviated from the SM predictions as follows: [17]

$$\frac{\text{BR}(B_s \rightarrow \mu^+ \mu^-)}{\text{BR}(B_s \rightarrow \mu^+ \mu^-)_{\text{SM}}} = \left| 1 - \frac{(C_L^{dB_s})_{\mu\mu}}{g_{SM}^2 \eta_Y Y_0(x_t) (V_{CKM})_{tb}^* (V_{CKM})_{ts}} \right|^2, \quad (49)$$

where $g_{SM}^2 = \sqrt{2} G_F \alpha / (\pi \sin^2 \theta_W)$ and $\eta_Y = 1.012$ [39] are defined. $(C_L^{dB_s})_{\mu\mu}$ is given by replacing A_{sd}^d with A_{bs}^d in $(C_L^l)_{\mu\mu}$. $\text{BR}(B \rightarrow \mu^+ \mu^-)$ can be also described by using A_{bd}^d and $(V_{CKM})_{td}$ instead of A_{bs}^d and $(V_{CKM})_{ts}$ in Eq. (49). Note that $(C_L^{dB_s})_{\mu\mu}$ depends on $A_{\mu\mu}^l$ as well.

Fig. 7 shows our predictions for the deviation of $\text{BR}(B_s \rightarrow \mu^+ \mu^-)$ and $\text{BR}(B \rightarrow \mu^+ \mu^-)$ in the each case with $\Lambda_{Z'} = 1400$ TeV (left) and $\Lambda_{Z'} = 500$ TeV (right). The deviation of $\text{BR}(B_s \rightarrow \mu^+ \mu^-)$ is large, compared to the one of $\text{BR}(B \rightarrow \mu^+ \mu^-)$, but it is at most a few % even in the 500 TeV $\Lambda_{Z'}$ case.

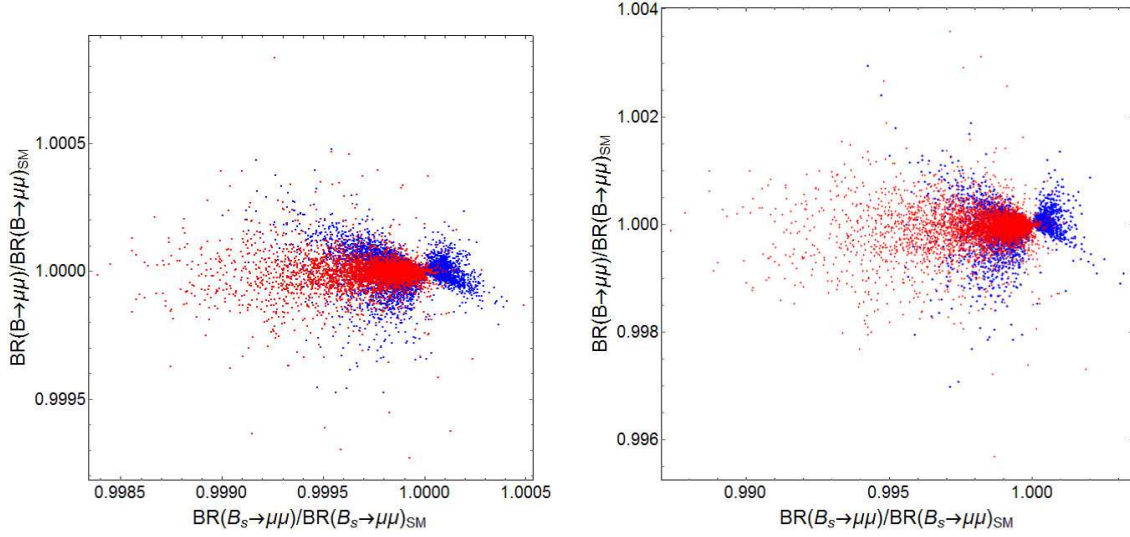


Figure 7: Our predictions for the deviation of $\text{BR}(B_s \rightarrow \mu^+ \mu^-)$ and $\text{BR}(B \rightarrow \mu^+ \mu^-)$ with $\Lambda_{Z'} = 1400$ TeV (left) and $\Lambda_{Z'} = 500$ TeV (right). The coefficients of higher-dimensional operators satisfy $|\epsilon c_{ij}^d| < 10^{-2}$ (red) and $|\epsilon c_{ij}^d| < 10^{-3}$ (blue). In these figures, the constraint, $|\delta\epsilon_K| \leq 0.3$, is assigned.

3.3 Flavor violating processes in μ decay

The tree-level FCNCs of Z' predict the LFV decays. Depending on the sizes of the coefficients of higher-dimensional operators, all elements of the FCNCs could be $\mathcal{O}(1)$, and then the LFV processes, which face the stringent experimental constraints, are important in our model; that is, $\mu \rightarrow 3e$ and μ - e conversions in nuclei should be taken into account. Note that $\mu \rightarrow e\gamma$ is one of the relevant processes, but it is suppressed in our model, because of the heavy Z' and the loop suppression.

3.3.1 $\mu \rightarrow 3e$

First, let us discuss $\mu \rightarrow 3e$ in our model. The LFV is caused by the following 4-Fermi interactions:

$$\mathcal{H}^{\mu \rightarrow 3e} = C_L^{3e} (\bar{e}_L \gamma^\mu \mu_L) (\bar{e}_L \gamma^\mu e_L) + C_R^{3e} (\bar{e}_L \gamma^\mu \mu_L) (\bar{e}_R \gamma^\mu e_R), \quad (50)$$

where the coefficients are given by

$$C_L^{3e} = A_{e\mu}^l \left\{ \frac{A_{ee}^l}{\Lambda_{Z'}^2} - \frac{\cos 2\theta_W}{2} \frac{1}{\Lambda_Z^2} \right\}, \quad (51)$$

$$C_R^{3e} = A_{e\mu}^l \left\{ \frac{1}{\Lambda_{Z'}^2} + \sin^2 \theta_W \frac{1}{\Lambda_Z^2} \right\}. \quad (52)$$

The branching ratio of $\mu \rightarrow 3e$ can be evaluated, ignoring the Z' contribution to $\mu \rightarrow e\bar{\nu}\nu$:

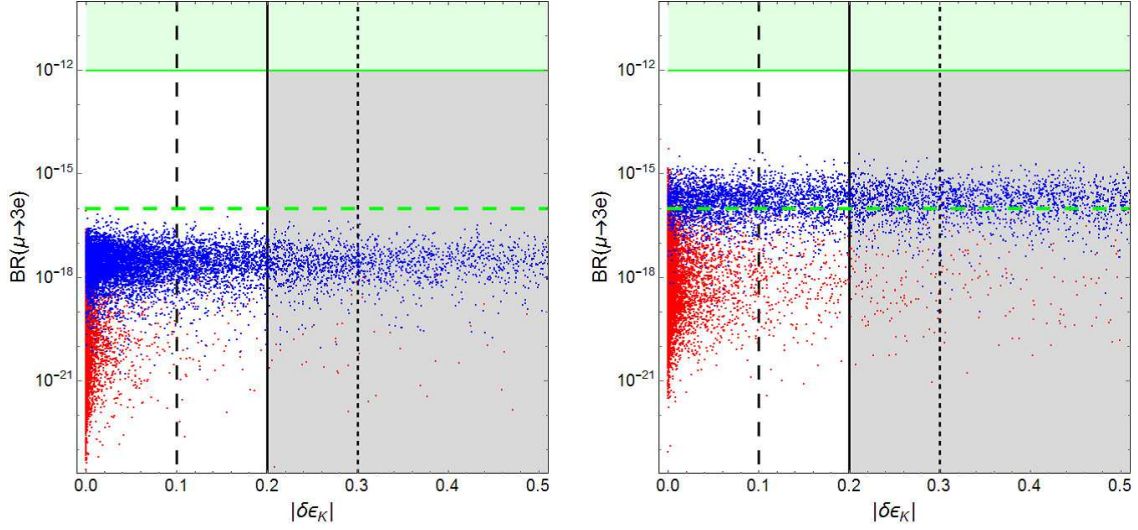


Figure 8: Our predictions for the deviation of $\text{BR}(\mu \rightarrow 3e)$ with $\Lambda_{Z'} = 1400$ TeV (left) and $\Lambda_{Z'} = 500$ TeV (right). The coefficients of higher-dimensional operators satisfy $|\epsilon c_{ij}^d| < 10^{-2}$ (red) and $|\epsilon c_{ij}^d| < 10^{-3}$ (blue). The green region is excluded by the SINDRUM experiment [40] and the green dashed line is the future prospected bound [41].

$$\text{BR}(\mu \rightarrow 3e) = \frac{m_\mu^5}{1536 \pi^3 \Gamma_\mu} \left(2 |C_L^{3e}|^2 + |C_R^{3e}|^2 \right) \quad (53)$$

$$\simeq 5.8 \times 10^{-18} \left(\frac{1400 \text{ TeV}}{\Lambda_{Z'}} \right)^4 \left(\frac{|A_{\mu e}^l|}{0.04} \right)^2, \quad (54)$$

where m_μ and Γ_μ are mass and total decay width for μ , respectively.

This LFV process has been investigated at the SINDRUM experiment: $\text{BR}(\mu \rightarrow 3e) < 1.0 \times 10^{-12}$ [40]. The coming experiment will reach $\mathcal{O}(10^{-16})$ [41]. Fig. 8 shows the correlation between $\delta(\epsilon_K)$ and $\text{BR}(\mu \rightarrow 3e)$, setting $\Lambda_{Z'} = 1400$ TeV (left) and $\Lambda_{Z'} = 500$ TeV (right). The green region is excluded by the SINDRUM experiment [40] and the dashed green line corresponds to the expected upper bound in the Mu3e experiment [41]. According to the figures, we can expect that $\text{BR}(\mu \rightarrow 3e)$ is less than $\mathcal{O}(10^{-15})$, as far as $\Lambda_{Z'} > 500$ TeV. When $\Lambda_{Z'}$ is 500 TeV which correspond to $M_{Z'} \simeq 36$ TeV, $\text{BR}(\mu \rightarrow 3e)$ is about 3.5×10^{-16} and can exceed the future sensitivity. Note that $|\delta\epsilon_K|$ is also enhanced in this case, as shown in Fig. 4.

3.3.2 μ - e conversion

The μ - e conversions in nuclei are also predicted by our Z' interaction. Now, we assume that the coherent conversion, in which the final state is the same as the initial, is dominant

and then we concentrate on the contributions derived from the operators,

$$\mathcal{H}^{\mu-e} = C_q^{\mu-e} (\bar{q} \gamma_\mu q) (\bar{e}_L \gamma^\mu \mu_L), \quad (55)$$

where the coefficients are given by

$$C_u^{\mu-e} = A_{e\mu}^l \left\{ \left(\frac{1}{4} - \frac{2}{3} \sin^2 \theta_W \right) \frac{1}{\Lambda_Z^2} \right\}, \quad (56)$$

$$C_d^{\mu-e} = -A_{e\mu}^l \left\{ \frac{A_{dd}^d + 1}{2\Lambda_{Z'}^2} + \left(\frac{1}{4} - \frac{1}{3} \sin^2 \theta_W \right) \frac{1}{\Lambda_Z^2} \right\}. \quad (57)$$

The conversion rate of muon ω_{conv} is

$$\omega_{\text{conv}} = 4m_\mu^5 \left| (2C_u^{\mu-e} + C_d^{\mu-e}) V^{(p)} + (C_u^{\mu-e} + 2C_d^{\mu-e}) V^{(n)} \right|^2, \quad (58)$$

where $V^{(p)}$ and $V^{(n)}$ are overlap integrals which depend on the nucleus species. The branching ratio of the μ - e conversion is

$$\begin{aligned} \text{BR}(\mu N \rightarrow e N) &= \frac{\omega_{\text{conv}}}{\omega_{\text{capt}}} \\ &\simeq 4.0 \times 10^{-17} (1.4 \times 10^{-17}) \left(\frac{1400 \text{ TeV}}{\Lambda_{Z'}} \right)^4 \left(\frac{|A_{\mu e}^l|}{0.04} \right)^2, \end{aligned} \quad (59)$$

where ω_{capt} is the muon capture rate. The overlap integrals $V^{(p)}$ and $V^{(n)}$ and the muon capture rate ω_{capt} have been calculated in Ref. [42] for the each nucleus species. We also show the typical value of $\text{BR}(\mu \text{Au} \rightarrow e \text{Au})$ ($\text{BR}(\mu \text{Al} \rightarrow e \text{Al})$) in our model.

Fig. 9 shows the correlations on $\delta\epsilon_K$ and the μ - e conversions. The green region is excluded by the SINDRUM experiment [43]. The dashed green lines are the future prospects for $\text{BR}(\mu \text{Al} \rightarrow e \text{Al})$. In these observables, the upper limits are depicted in Fig. 9, depending on the sizes of ϵ and $\Lambda_{Z'}$: $\text{BR}(\mu N \rightarrow e N) < \mathcal{O}(10^{-15})$. Although these results are much below the current experimental limit, there is a chance to reach the future sensitivity of the COMET-II experiment [44, 45] in the mode of $\mu \text{Al} \rightarrow e \text{Al}$: $\text{BR}(\mu \text{Al} \rightarrow e \text{Al}) \simeq 10^{-15}$ when $\Lambda_{Z'}$ is set to 500 TeV.

3.4 Contributions to LFV τ decays

Finally, let us discuss LFV τ decays: $\tau \rightarrow l_i l_j \bar{l}_k$ and $\tau \rightarrow l_i P^0$, where P^0 denotes neutral mesons, $P^0 = \pi^0, K_S$, in this section. To begin with, we discuss the leptonic decay, $\tau \rightarrow l_i l_j \bar{l}_k$. This decay is caused by the following 4-Fermi interactions similar to Eq. (50):

$$\mathcal{H}^{\tau \rightarrow 3l} = C_{L\,ijk}^{3l} (\bar{l}_{Li} \gamma^\mu \tau_L) (\bar{l}_{Lj} \gamma_\mu l_{Lk}) + C_{R\,ijk}^{3l} (\bar{l}_{Li} \gamma^\mu \tau_L) (\bar{l}_{Rj} \gamma^\mu l_{Rk}), \quad (60)$$

where the coefficients are given by

$$C_{L\,ijk}^{3l} = A_{i\tau}^l \left\{ \frac{A_{jk}^l}{\Lambda_{Z'}^2} - \frac{\cos 2\theta_W}{2} \frac{\delta_{jk}}{\Lambda_Z^2} \right\}, \quad (61)$$

$$C_{R\,ijk}^{3l} = A_{i\tau}^l \delta_{jk} \left\{ \frac{1}{\Lambda_{Z'}^2} + \sin^2 \theta_W \frac{1}{\Lambda_Z^2} \right\}. \quad (62)$$

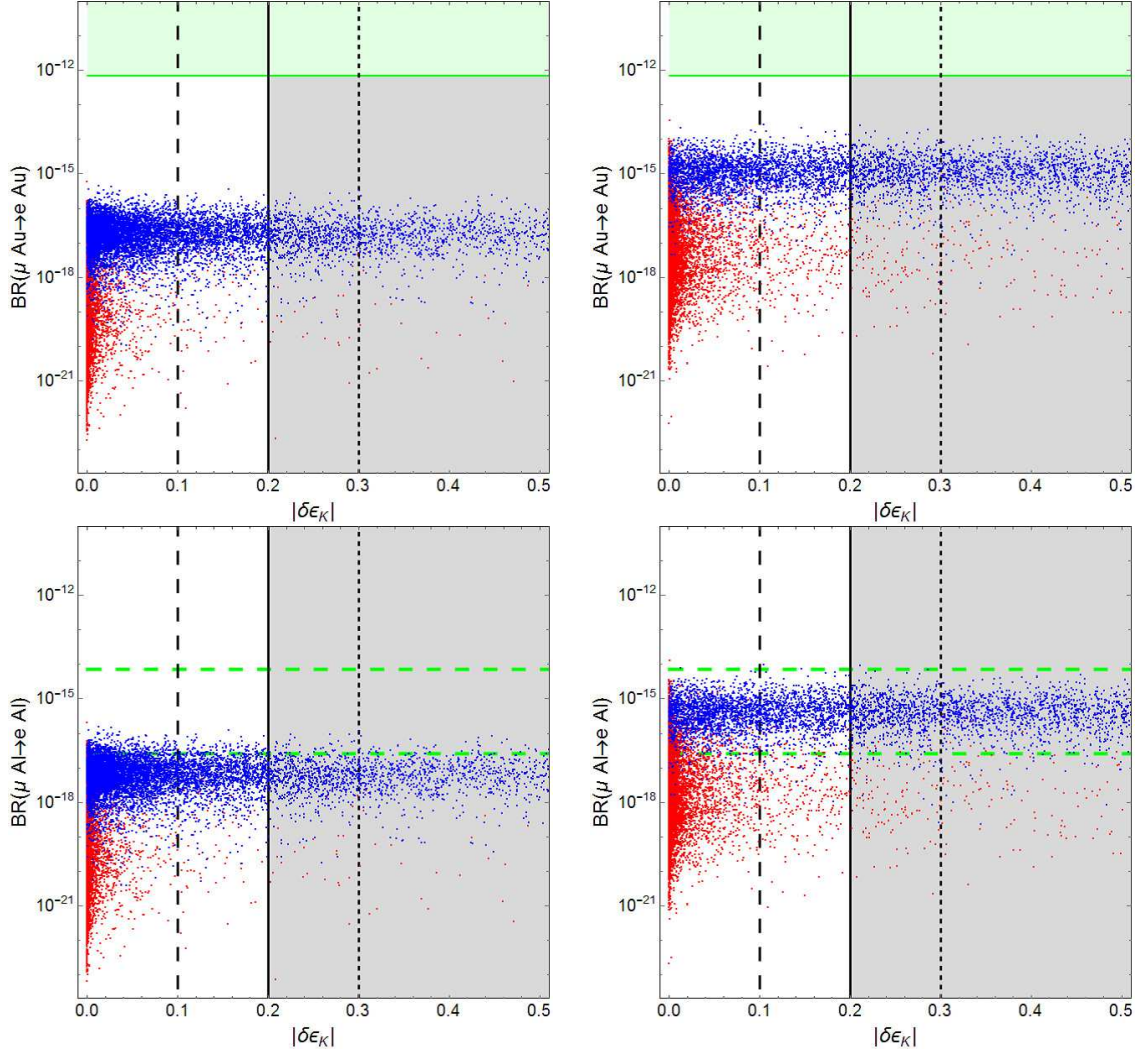


Figure 9: Our predictions for $\text{BR}(\mu \text{Au} \rightarrow e \text{Au})$ (upper panels) and $\text{BR}(\mu \text{Al} \rightarrow e \text{Al})$ (lower panels). We set $\Lambda_{Z'} = 1400$ TeV in left two panels and $\Lambda_{Z'} = 500$ TeV in right two panels. The coefficients of higher-dimensional operators satisfy $|\epsilon c_{ij}^d| < 10^{-2}$ (red) and $|\epsilon c_{ij}^d| < 10^{-3}$ (blue). In the upper panels, green region shows the experimental bound [43]. In the lower panels, two green dashed lines show future sensitivity from COMET-I (upper one) and COMET-II (lower one) experiment [44, 45].

In LFV τ decays, there are many modes, e.g. $\tau \rightarrow 3\mu$, $\tau \rightarrow \mu^- e^+ e^-$, $\tau \rightarrow e^+ \mu^- \mu^-$ and so on. The branching ratios for some of these modes can be estimated by changing $m_\mu \rightarrow m_\tau$, $\Gamma_\mu \rightarrow \Gamma_\tau$ and $C_{L,R}^{3e} \rightarrow C_{L,R}^{3l}$ in Eq. (53). In the case that there are three

different charged leptons in final state, the branching ratio for $\tau \rightarrow l_i l_j \bar{l}_k$ is [46]

$$\text{BR}(\tau \rightarrow l_i l_j \bar{l}_k) = \frac{m_\tau^5}{1536 \pi^3 \Gamma_\tau} \left(\left| C_{L_{ijk}}^{3l} + C_{L_{jik}}^{3l} \right|^2 + \left| C_{R_{ijk}}^{3l} \right|^2 + \left| C_{R_{jik}}^{3l} \right|^2 \right). \quad (63)$$

We show the typical values of branching ratios for all decay modes of $\tau \rightarrow l_i l_j \bar{l}_k$ in Table 3 and we found that these modes are extremely smaller than the experimental bounds [15,47] in our model.

Next, let us discuss $\tau \rightarrow l_i \pi^0$ and $\tau \rightarrow l_i K_S$. These decays are caused by the following interactions:

$$\mathcal{H}^{\tau \rightarrow l P^0} = C_{L_{ijk}}^{l P^0} (\bar{l}_{L_i} \gamma^\mu \tau_L) (\bar{q}_{L_j} \gamma_\mu q_{L_k}) + C_{R_{ijk}}^{l P^0} (\bar{l}_{L_i} \gamma^\mu \tau_L) (\bar{q}_{R_j} \gamma_\mu q_{R_k}), \quad (64)$$

where the coefficients are similar to Eq. (33):

$$C_{I_{ijk}}^{l P^0} = A_{i\tau}^l \left\{ \frac{(Q_I^q)_{jk}}{\Lambda_{Z'}^2} + \frac{\delta_{jk}}{\Lambda_Z^2} (\tau_I^q - Q_e^q \sin^2 \theta_W) \right\}. \quad (65)$$

The branching ratios of $\tau \rightarrow l_i \pi^0$ and $\tau \rightarrow l_i K_S^0$ are evaluated by the following expression [46]:

$$\text{BR}(\tau \rightarrow l_i \pi^0) = \frac{\text{BR}(\tau \rightarrow \nu_\tau \pi^-)}{16 |(V_{CKM})_{ud}|^2 G_F^2} \times \left(|C_{L_{iuv}}^{l P^0} - C_{R_{iuv}}^{l P^0} - C_{L_{idd}}^{l P^0} + C_{R_{idd}}^{l P^0}|^2 \right), \quad (66)$$

$$\text{BR}(\tau \rightarrow l_i K_S) = \frac{\text{BR}(\tau \rightarrow \nu_\tau K^-)}{16 |(V_{CKM})_{us}|^2 G_F^2} \times \left(|C_{R_{isd}}^{l P^0} - C_{R_{ids}}^{l P^0}|^2 \right), \quad (67)$$

where $\text{BR}(\tau \rightarrow \nu_\tau \pi^-) = 0.1083$ and $\text{BR}(\tau \rightarrow \nu_\tau K^-) = 0.007$ [15].

We summarize the typical values of each branching ratio for $\tau \rightarrow l_i P^0$ and each experimental bound [15] in Table 3. We see that these decay modes are also smaller than the experimental bounds. Note that $\text{BR}(\tau \rightarrow e P^0)$ is smaller than $\text{BR}(\tau \rightarrow \mu P^0)$ because this type of branching ratio is proportional to $|A_{i\tau}^l|^2$ and roughly speaking, $|A_{e\tau}^l| < |A_{\mu\tau}^l|$.

4 Summary

The grand unification is one of the attractive hypotheses to solve the mystery of our nature. The SO(10) GUT elegantly explains the origin of the SM gauge groups and the minimal setup shows that all matters except Higgs fields can be unified into a **16**-representational field in the each generation surprisingly. Our nature, however, is not so simple. The hierarchical structure of the fermions exists in the each sector, (i.e. up-type, down-type, and leptonic Yukawa couplings), but the observed values unfortunately seem to dislike the unification of the Yukawa couplings. In Ref. [10], we propose a SO(10)-GUT model, introducing **10**-representational matter fields, in order to realize the realistic Yukawa couplings. In this model, the SM fields are given by the linear combination of the parts of the **10**- and **16**-representational fields, and especially the mass hierarchy between

τ decay mode	value of BR	exp. bound ($\times 10^{-8}$) [15, 47]
$e^-e^+e^-$	1.2×10^{-18}	< 2.7
$e^-\mu^+\mu^-$	4.2×10^{-19}	< 2.7
$e^+\mu^-\mu^-$	1.5×10^{-18}	< 1.7
$\mu^-e^+e^-$	3.7×10^{-15}	< 1.8
$\mu^+e^-e^-$	2.8×10^{-22}	< 1.5
$\mu^-\mu^+\mu^-$	2.7×10^{-15}	< 2.1
$e^-\pi^0$	2.2×10^{-19}	< 8.0
$\mu^-\pi^0$	1.2×10^{-15}	< 11
$e^-K_s^0$	1.2×10^{-21}	< 2.6
$\mu^-K_s^0$	6.6×10^{-18}	< 2.3

Table 3: The typical values of each τ decay mode. In this table, we use $\Lambda_{Z'} = 1.4 \times 10^3$ TeV and typical values of A_{ij}^d and A_{ij}^l .

top and bottom quarks is achieved by the mixing. Although we have to expect additional contributions such as higher-dimensional operators to the fermion mass matrices, we have successfully reproduced the realistic Yukawa couplings in this paper.

The important and interesting feature of our model is to predict the flavor violating couplings of Z' . SO(10) predicts an extra U(1)' symmetry. In our scenario, the matter fields are given by the two different fields of SO(10), which carry different U(1)' charges. Then, the flavor violating Z' interaction is induced by the spontaneous U(1)' symmetry breaking, and we can expect that the Z' couplings are related to the Yukawa couplings, such as the mass hierarchy and the mixing. In fact, we find that the flavor violating Z' couplings, denoted by $A_{ij}^{d,l}$, depend on the fermion masses and the CKM matrix, and we derive the explicit forms of $A_{ij}^{d,l}$, although the unknown parameters appear according to the higher-dimensional operators. Interestingly, we see that there are some correlations among the flavor violating Z' couplings. For example, A_{ij}^d (A_{ij}^l) are linear to m_i^d and m_j^d (m_i^l and m_j^l), so that A_{bs}^d tends to be large and A_{ij}^l/A_{ij}^d is approximately estimated as $m_i^l m_j^l / (m_i^d m_j^d)$, in the limit that $\epsilon \rightarrow 0$.

In this paper, we especially investigate the flavor physics relevant to our FCNCs. $A_{ij}^{d,l}$, actually, could be $\mathcal{O}(1)$, depending on the size of the coefficients of higher-dimensional operators. Then, ϵ_K is the most sensitive to our model. Besides, the large (b , s) element of the Z' coupling predicts relatively large deviations of ΔM_{B_s} and B_s decay.

Moreover, we find that there are correlations between the flavor violation in the quark sector and LFV. In the LFV, the stringent constraints come from the LFV μ decays, such as μ - e conversion and $\mu \rightarrow 3e$. They are expected to be developed near future, so that our model could be tested, for instance, in the COMET and Mu2e experiments. As

we see Fig. 9, our prediction could reach the future prospect of the COMET without conflict with ϵ_K , if Z' scale is $\mathcal{O}(100)$ TeV. Other future experiments for μ - e conversion are planned [48–50], and our model can be tested if their sensitivities reach $\mathcal{O}(10^{-15})$. If we assume that the extra $U(1)'$ is radiatively broken around the SUSY scale, Z' scale would be $\mathcal{O}(100)$ TeV to realize 125 GeV Higgs in the high-scale SUSY scenario. Then, it is implied that our SUSY model can be tested indirectly, even though the SUSY scale is much higher than the energy scale reached by the LHC.

Before closing our discussion, let us give some comments on the other observables in flavor physics. In our model, all elements of the tree-level FCNCs involving Z' could be large in principle, so that all observables may be relevant to our model. One of the processes that recently attract attention is the direct CP violation in $K \rightarrow \pi\pi$. As pointed out in Ref. [51, 52], the SM prediction of ϵ'/ϵ is deviated from the experimental results, according to the lattice QCD calculation. Another interesting process would be $b \rightarrow s$ transition, such as $B \rightarrow K ll$, which is slightly deviated from the SM prediction [53, 54]. The new physics interpretations are given by, e.g. Ref. [55], and summarized in Refs. [56, 57]. In those processes, our predictions will depart from the SM predictions as well, so that it would be interesting to discuss if our model can resolve the discrepancies, although relatively low Z' scale should be assumed. This work may be done elsewhere in the future.

Acknowledgments

This work is supported by Grant-in-Aid for Scientific research from the Ministry of Education, Science, Sports, and Culture (MEXT), Japan, No.16H00867 and 16H06492 (for J.H.), and National Research Foundation of Korea (NRF) Research Grant NRF-2015R1A2A1A05001869 (for Y.M.). The work of J.H. is also supported by World Premier International Research Center Initiative (WPI Initiative), MEXT, Japan. The work of Y.S. is supported by the Japan Society for the Promotion of Science (JSPS) Research Fellowships for Young Scientists, No. 16J08299.

A RG equations for the $\Delta F = 2$ processes

The one-loop RG equation for \tilde{Q}_1^q is given by

$$\mu \frac{d}{d\mu} \tilde{C}_1^q = -\frac{\alpha_s}{2\pi} \left(\frac{3}{N_c} - 3 \right) \tilde{C}_1^q. \quad (68)$$

Using the one-loop description of the RG running of α_s , we can estimate the one-loop Wilson coefficients in the each process: for the K - \bar{K} mixing,

$$\tilde{C}_1^K(m_K) = \left(\frac{\alpha_s(m_c)}{\alpha_s(m_K)} \right)^{\frac{2}{9}} \left(\frac{\alpha_s(m_b)}{\alpha_s(m_c)} \right)^{\frac{6}{25}} \left(\frac{\alpha_s(m_t)}{\alpha_s(m_b)} \right)^{\frac{6}{23}} \left(\frac{\alpha_s(M_{Z'})}{\alpha_s(m_t)} \right)^{\frac{2}{7}} \tilde{C}_1^K(M_{Z'}), \quad (69)$$

and for the $B_{(s)}\text{-}\overline{B}_{(s)}$ mixing,

$$\tilde{C}_1^{B_{(s)}}(m_b) = \left(\frac{\alpha_s(m_t)}{\alpha_s(m_b)}\right)^{\frac{6}{23}} \left(\frac{\alpha_s(M_{Z'})}{\alpha_s(m_t)}\right)^{\frac{2}{7}} \tilde{C}_1^{B_{(s)}}(M_{Z'}). \quad (70)$$

B Functions

The functions which appear in the $K\text{-}\overline{K}$ and $B_{(s)}\text{-}\overline{B}_{(s)}$ mixing are given by

$$S_0(x) = \frac{4x - 11x^2 + x^3}{4(1-x)^2} - \frac{3x^3 \log x}{2(1-x)^3}, \quad (71)$$

$$S(x, y) = \frac{-3xy}{4(y-1)(x-1)} - \frac{xy(4-8y+y^2) \log y}{4(y-1)^2(x-y)} + \frac{xy(4-8x+x^2) \log x}{4(x-1)^2(x-y)}. \quad (72)$$

The function for the short-distance contribution to $K_L \rightarrow \pi \bar{\nu} \nu$ is defined as

$$X(x) = \frac{x}{8} \left\{ \frac{x+2}{x-1} + \frac{3x-6}{(x-1)^2} \log x \right\}. \quad (73)$$

The function for $B_{s(d)} \rightarrow \mu^+ \mu^-$ is defined as

$$Y_0(x) = \frac{x}{8} \left\{ \frac{x-4}{x-1} + \frac{3x}{(x-1)^2} \ln x \right\}. \quad (74)$$

References

- [1] H. Georgi, AIP Conf. Proc. **23**, 575 (1975); H. Fritzsch and P. Minkowski, Annals Phys. **93**, 193 (1975).
- [2] H. Georgi and C. Jarlskog, Phys. Lett. B **86**, 297 (1979).
- [3] J. R. Ellis and M. K. Gaillard, Phys. Lett. B **88**, 315 (1979); G. Lazarides, Q. Shafi and C. Wetterich, Nucl. Phys. B **181**, 287 (1981).
- [4] S. M. Barr, Phys. Rev. D **24**, 1895 (1981).
- [5] N. Arkani-Hamed and S. Dimopoulos, JHEP **0506**, 073 (2005) [hep-th/0405159]; G. F. Giudice and A. Romanino, Nucl. Phys. B **699**, 65 (2004) [Erratum-ibid. B **706**, 65 (2005)] [hep-ph/0406088]; N. Arkani-Hamed, S. Dimopoulos, G. F. Giudice and A. Romanino, Nucl. Phys. B **709**, 3 (2005) [hep-ph/0409232]; J. D. Wells, Phys. Rev. D **71**, 015013 (2005) [hep-ph/0411041]; G. F. Giudice and A. Strumia, Nucl. Phys. B **858**, 63 (2012) [arXiv:1108.6077 [hep-ph]]; L. J. Hall and Y. Nomura, JHEP **1201**,

- 082 (2012) [arXiv:1111.4519 [hep-ph]]; M. Ibe and T. T. Yanagida, Phys. Lett. B **709**, 374 (2012) [arXiv:1112.2462 [hep-ph]]; M. Ibe, S. Matsumoto and T. T. Yanagida, Phys. Rev. D **85**, 095011 (2012) [arXiv:1202.2253 [hep-ph]]; N. Arkani-Hamed, A. Gupta, D. E. Kaplan, N. Weiner and T. Zorawski, arXiv:1212.6971 [hep-ph].
- [6] H. Abe, T. Kobayashi and Y. Omura, Phys. Rev. D **76**, 015002 (2007) [hep-ph/0703044 [HEP-PH]].
- [7] H. Abe, J. Kawamura and H. Otsuka, PTEP **2013**, 013B02 (2013) [arXiv:1208.5328 [hep-ph]].
- [8] J. L. Feng and D. Sanford, Phys. Rev. D **86**, 055015 (2012) [arXiv:1205.2372 [hep-ph]].
- [9] H. Baer, V. Barger, P. Huang, A. Mustafayev and X. Tata, Phys. Rev. Lett. **109**, 161802 (2012) [arXiv:1207.3343 [hep-ph]].
- [10] J. Hisano, Y. Muramatsu, Y. Omura and M. Yamanaka, Phys. Lett. B **744**, 395 (2015) [arXiv:1503.06156 [hep-ph]].
- [11] J. Hisano, D. Kobayashi and N. Nagata, Phys. Lett. B **716**, 406 (2012) [arXiv:1204.6274 [hep-ph]]; J. Hisano, D. Kobayashi, Y. Muramatsu and N. Nagata, Phys. Lett. B **724** (2013) 283 [arXiv:1302.2194 [hep-ph]]; J. Hisano, T. Kuwahara and Y. Omura, Nucl. Phys. B **898** (2015) 1 [arXiv:1503.08561 [hep-ph]]; B. Bajc, J. Hisano, T. Kuwahara and Y. Omura, Nucl. Phys. B **910**, 1 (2016) [arXiv:1603.03568 [hep-ph]].
- [12] K. G. Chetyrkin, J. H. Kuhn and M. Steinhauser, Comput. Phys. Commun. **133**, 43 (2000) [hep-ph/0004189].
- [13] H. Arason, D. J. Castano, B. Keszthelyi, S. Mikaelian, E. J. Piard, P. Ramond and B. D. Wright, Phys. Rev. D **46**, 3945 (1992).
- [14] S. P. Martin and M. T. Vaughn, Phys. Lett. B **318**, 331 (1993) [hep-ph/9308222].
- [15] K. A. Olive *et al.* [Particle Data Group], Chin. Phys. C **38**, 090001 (2014).
- [16] Web site of CKMfitter group (EPS-HEP 2015 conference)
http://ckmfitter.in2p3.fr/www/results/plots_eps15/num/ckmEval_results_eps15.html
- [17] A. J. Buras, F. De Fazio and J. Girrbach, JHEP **1302**, 116 (2013) [arXiv:1211.1896 [hep-ph]].
- [18] Jack Laiho, E. Lunghi and Ruth S. Van de Water, Phys. Rev. D **81**, 034503 (2010) [arXiv:0910.2928 [hep-ph]].

See also the latest values in <http://www.latticeaverages.org>.

- [19] J. Brod and M. Gorbahn, Phys. Rev. Lett. **108**, 121801 (2012) [arXiv:1108.2036 [hep-ph]].
- [20] A. J. Buras, M. Jamin and P. H. Weisz, Nucl. Phys. B **347**, 491 (1990).
- [21] J. Brod and M. Gorbahn, Phys. Rev. D **82**, 094026 (2010) [arXiv:1007.0684 [hep-ph]].
- [22] J. Charles, S. Descotes-Genon, Z. Ligeti, S. Monteil, M. Papucci and K. Trabelsi, Phys. Rev. D **89**, no. 3, 033016 (2014) [arXiv:1309.2293 [hep-ph]].
- [23] A. Bazavov *et al.* [Fermilab Lattice and MILC Collaborations], Phys. Rev. D **93**, no. 11, 113016 (2016) [arXiv:1602.03560 [hep-lat]].
- [24] J. K. Ahn *et al.* [E391a Collaboration], Phys. Rev. D **81**, 072004 (2010) [arXiv:0911.4789[hep-ex]].
- [25] A. V. Artamonov *et al.* [E949 Collaboration], Phys. Rev. D **79**, 092004 (2009) [arXiv:0903.0030[hep-ex]].
- [26] A. J. Buras, D. Buttazzo, J. Girrbach-Noe and R. Knegjens, JHEP **1511**, 033 (2015) [arXiv:1503.02693 [hep-ph]].
- [27] F. Mescia and C. Smith, Phys. Rev. D **76**, 034017 (2007) [arXiv:0705.2025 [hep-ph]].
- [28] J. Brod, M. Gorbahn and E. Stamou, Phys. Rev. D **83**, 034030 (2011) [arXiv:1009.0947 [hep-ph]].
- [29] G. Ishidori and R. Unterdorfer, JHEP **01**, 009 (2004) [hep-ph/0311084].
- [30] A. J. Buras, R. Fleischer, S. Recksiegel and F. Schwab, Nucl. Phys. B **697**, 133 (2004) [hep-ph/0402112].
- [31] M. Gorbahn and U. Haisch, Phys. Rev. Lett. **97**, 122002 (2006) [hep-ph/0605203].
- [32] D. Ambrose, *et al.* [BNL E871 Collaboration], Phys. Rev. Lett. **81**, 5734 (1998) [hep-ex/9811038].
- [33] A. Alavi-Harati, *et al.* [KTeV collaboration], Phys. Rev. Lett. **93**, 021805 (2003) [hep-ex/0309072].
- [34] A. Alavi-Harati, *et al.* [KTeV collaboration], Phys. Rev. Lett. **84**, 5279 (2000) [hep-ex/0001006].
- [35] F. Mescia, C. Smith and S. Trine, JHEP **0608**, 088 (2006) [hep-ph/0606081].
- [36] E. Abouzaid *et al.* [KTeV Collaboration], Phys. Rev. Lett. **100**, 131803 (2008) [arXiv:0711.3472[hep-ex]].

- [37] V. Khachatryan *et al.* [CMS and LHCb Collaborations], *Nature* **522**, 68 (2015) [arXiv:1411.4413 [hep-ex]].
- [38] C. Bobeth, M. Gorbahn, T. Hermann, M. Misiak, E. Stamou and M. Steinhauser, *Phys. Rev. Lett.* **112**, 101801 (2014) [arXiv:1311.0903 [hep-ph]].
- [39] G. Buchalla and A. J. Buras, *Nucl. Phys. B* **548**, 309 (1999) [hep-ph/9901288].
- [40] U. Bellgardt *et al.* [SINDRUM Collaboration], *Nucl. Phys. B* **299**, 1 (1988).
- [41] A. Blondel, A. Bravar, M. Pohl, S. Bachmann, N. Berger, M. Kiehn, A. Schoning and D. Wiedner *et al.*, arXiv:1301.6113 [physics.ins-det].
- [42] R. Kitano, M. Koike and Y. Okada, *Phys. Rev. D* **66**, 096002 (2002) [Erratum-ibid. *D* **76**, 059902 (2007)] [hep-ph/0203110].
- [43] W. H. Bertl *et al.* [SINDRUM II Collaboration], *Eur. Phys. J. C* **47**, 337 (2006).
- [44] Y. Kuno [COMET Collaboration], *PTEP* **2013**, 022C01 (2013).
- [45] COMET Collaboration,
(Available at: http://comet.kek.jp/Documents_files/IPNS-Review-2014.pdf)
- [46] P. Langacker and M. Plumacher, *Phys. Rev. D.* **62**, 013006 (2000) [hep-ph/0001204].
- [47] K. Hayasaka, K. Inami, Y. Miyazaki, K. Arinstein, V. Aulchenko, T. Aushev, A. M. Bakich and A. Bay *et al.*, *Phys. Lett. B* **687**, 139 (2010) [arXiv:1001.3221 [hep-ex]].
- [48] H. Natori [DeeMe Collaboration], *Nucl. Phys. Proc. Suppl.* **248-250**, 52 (2014).
- [49] Mu2e Collaboration, FERMILAB-PROPOSAL-0973
(Available at: <http://mu2e-docdb.fnal.gov/cgi-bin/ShowDocument?docid=388>).
- [50] PRISM Collaboration,
(Available at: <http://www-ps.kek.jp/jhf-np/LOIlist/pdf/L25.pdf>).
- [51] Z. Bai *et al.* [RBC and UKQCD Collaborations], *Phys. Rev. Lett.* **115**, no. 21, 212001 (2015) [arXiv:1505.07863 [hep-lat]].
- [52] A. J. Buras, M. Gorbahn, S. Jäger and M. Jamin, *JHEP* **1511**, 202 (2015) [arXiv:1507.06345 [hep-ph]].
- [53] R. Aaij *et al.* [LHCb Collaboration], *Phys. Rev. Lett.* **111**, 191801 (2013) doi:10.1103/PhysRevLett.111.191801 [arXiv:1308.1707 [hep-ex]].
- [54] R. Aaij *et al.* [LHCb Collaboration], *Phys. Rev. Lett.* **113**, 151601 (2014) [arXiv:1406.6482 [hep-ex]].

- [55] S. Descotes-Genon, J. Matias and J. Virto, Phys. Rev. D **88**, 074002 (2013) [arXiv:1307.5683 [hep-ph]].
- [56] W. Altmannshofer and D. M. Straub, Eur. Phys. J. C **75**, no. 8, 382 (2015) [arXiv:1411.3161 [hep-ph]].
- [57] S. Descotes-Genon, L. Hofer, J. Matias and J. Virto, JHEP **1606**, 092 (2016) [arXiv:1510.04239 [hep-ph]].